SEA SURFACE TEMPERATURE OF THE COASTAL ZONES OF FRANCE

Heat Capacity Mapping Mission - HCMM
Investigation n° 15
Progress Report n° 4

P.Y DESCHAMPS and R. FROUIN
Laboratoire d'Optique Atmosphérique - Université de Lille I

J. CASSANET and F. VERGER
Laboratoire de Géographie - Ecole Normale Supérieure

M. CREPON
Laboratoire d'Océanographie Physique - Muséum d'Histoire Naturelle

J.M. MONGET and L. WALD
Centre de Télédétection et d'Analyse des Milieux Naturels, Ecole des Mines.

(E81-10083) SEA SURFACE TEMPERATURE OF THE COASTAL ZONES OF FRANCE Progress Report (Lille Univ.) 94 p HC A05/MF A01 CSCL 08J
N81-13436
Unclas
G3/43 00083

August 1980

SEA SURFACE TEMPERATURE OF THE COASTAL ZONES OF FRANCE

Heat Capacity Mapping Mission - HCMM
Investigation n° 15
Progress Report n° 4

P.Y DESCHAMPS and R. FROUIN
Laboratoire d'Optique Atmosphérique - Université de Lille I

J. CASSANET and F. VERGER
Laboratoire de Géographie - Ecole Normale Supérieure

M. CREPON
Laboratoire d'Océanographie Physique - Muséum d'Histoire Naturelle

J.M. MONGET and L. WALD
Centre de Télédétection et d'Analyse des Milieux Naturels, Ecole des Mines.

August 1980

SUMMARY

ani

LIST OF ABREVIATIONS

AVHRR - Advanced Very High Resolution Radiometer on Tiros-N and NOAA-6 satellites.

CCT - Computer Compatible Tape.

CMS - Centre de Météorologie Spatiale.

CTAMN - Centre de Télédétection et d'Analyse des Milieux Naturels.

HCMM - Heat Capacity Mapping Mission.

HCMR - Heat Capacity Mapping Radiometer.

SST - Sea Surface Temperature.

VHRR - Very High Resolution Radiometer on NOAA-1 to 5 satellites.

1 - INTRODUCTION

The objectives of this investigation are to map the various thermal gradients in the coastal zones of France with regard to natural phenomena and man-made thermal effluents : to study and map the mesoscale thermal features in the English Channel, the Bay of Biscay and the North Western Mediterranean Sea ; to study and map the evolution of the thermal gradients generated by the main estuaries of the french coastal zones ; and to contribute to the modelling of diurnal heating of the sea surface and its influence on the oceanic surface layers.

The investigation is conducted by the followings : Dr P.Y. DESCHAMPS (Principal Investigator) and Dr M. CREPON, Mr J.M. MONGET and Professor F. VERGER (Co-Investigators).
Appendix A give related organizations and addresses.

This progress report is the last one before final report of the investigations. Results have been emphasized, while methods and problems have not been discussed.

2 - RESULTS

2.1. Residual flow through the Dover Strait

Time sequence of HCMM scenes allowed us to outline the influence of meteorological conditions on the residual current which flows to the N.E., from the British Channel into the North Sea, through the Dover Strait.. S.W. winds enhance this residual flow, and, as a result, the thermal effluent of the Rhine River is kept to the Dutch coast in a very narrow coastal band. N.E. winds contrary the residual flow which is slown down and deviated to the English coast : then the Rhine thermal effluent propagates offshore at a distance of up to 25 nautical miles. A close correlation exists between wind speed direction and the offshore width of the effluent.

2.2. Upwelling at the continental shelf break in the Bay of Biscay

HCMM data confirm the existence of a permanent upwelling at the continental shelf break in the Bay of Biscay. The upwelling is outlined by the appearance of cold water in summertime. This was previously mentionned from VHRR data. From HCMM scenes, a more complete description and interpretation of the upwelling has been obtained.

(1) The upwelling is probally permanent, but is enhanced by upwelled colder water in summertime when a seasonal thermocline is formed. On one occasion, january 16, 1979, warmer water appeared in wintertime at the shelf break (HCMM scene n° 265 - 1090) : this water is probally a "mediterranean" water, warmer and salted, flowing out of the mediterranean sea, from the Gibraltar Strait, into the Atlantic, at a depth of several hundred meters.

(2) Upwelling is enhanced after spring tides, which suggests that the basic mechanism for the upwelling is a tidal one. On two occasions after spring tides, august 25 and september 21, 1978, HCMM scenes (ID n° A-A0121 - 13260 and A-A0148 - 13320) show very similar patterns of cold water at the shelf break, with a maximum intensity between 48N-8E and 46.30N-5E where the tidal currents are at a maximum.

2.3. Mesoscale variability of the SST field.

Using VHRR and HCMR infrared digital data, a statistical two-dimensional analysis of the mesoscale variability of the SST field has been performed in order to characteristize the random properties of this field. The power law exponent, n, of the spatial variance density spectrum, $E(k) \sim k^{-n}$ k is wavenumber), is deduced from the computation of the structure function of the SST. The study was first started on VHRR/NOAA-5 in the range of scales 40-100 km. HCMR data allowed us to extend the study down to a scale of 3 km. In the range of scales 3-100 km, n was found to vary from 1.5 to 2.3, with a mean value of 1.8, over a study of 11 VHRR and 9 HCMM scenes. These values of n are of the order of the predicted values by the two-dimensional turbulence theories. However a discrepancy exists and we need further advanced theories to explain this experimental determination of the mesoscale SST variability.

The feasability of the spectral analysis in the range of scales 3-30 km was made possible by the only low noise level of the HCMR data. A detailed manuscript is given as Appendice B.

2.4. Duirnal heating

Daytime HCMR data occasionnaly exhibit warmer sea surface areas which extend over 10 to 100 km. The warming is of several °C and is easily detected on photographic products because the warmer areas have usually smooth boundaries and cannot be confused with the sharper oceanic thermal boundaries.

These warmer areas are interpretated as a large diurnal heating of the upper surface layer under low wind speed conditions. Evidence of that is supported by several arguments.

(1) Meteorological observations and analysis show that warmer areas are associated with low wind speed conditions - i.e. anticyclonic conditions or coastal breeze effects.

(2) Glitter - i.e. direct solar radiation reflected by the wavy sea surface towards the sensor - has been used to derive an equivalent wind speed from the HCMR visible channel, where feasible (observation must be close to the specular reflection of a flat sea). Warmer areas are always associated with changes in the glitter patterns and decreasing wind speeds.

(3) Warmer areas disappear on consecetuve nightime HCMR data.

Under these low wind speed conditions, turbulence induced in the surface layer by the wind stress is strongly reduced, and most of the solar radiation absorbed is stored without downwards propagation. Theoretical simulations using a radiative and heat transfer model have been performed and predict large heating rates in the upper meter, and a maximum heating of several °C in the upper layer which is confirmed by a few in-situ measurements. Large heating only occurs in a few tens of cm and is very rapidly destroyed by the nightime cooling.

ani

HCMR data allowed us to discover that a diurnal heating of more than 1° C could affect large areas. Frequencies of occurence are relativêly high in the Western Mediterranean Sea where more than 10 % of marine surface are affected one day or an other, while a large diurnal heating is very unlikely in the North Sea (only one scene). In such strongly affected areas, daytime satellite data could consequently give meaningless SST fields, and observations should be restricted to nightime, or early in the morning when the surface layer is the most homogeneous. A detailed manuscript is given as Appendice C.

3 - CONCLUSIONS

During the reporting period, HCMM photographic products proved to be very useful :

(1) to interpret the influence of wind direction on the mean residual flow through the Dover Strait,

(2) to understand the upwelling occuring at the continental shelf break in the Bay of Biscay, and its relation with tidal currents.

A multitemporal analysis of HCMM digital products is on progress

(1) to obtain a mean value of diurnal heatings observed in the Western Mediterranean Sea, during summer months,

(2) to obtain a quantitative assessment of the intensity of the shelf break upwelling in the Bay of Biscay as function of tidal conditions.

Appendix A

Permanent adresses and organizations of the investigators

Dr. M. CREPON
Laboratoire d'Océanographie Physique
Museum d'Histoire Naturelle
43, rue Cuvier
75231 PARIS Cedex 05 (France)

Dr. P.Y. DESCHAMPS
Laboratoire d'Optique Atmosphérique
Université des Sciences et Techniques
U.E.R. de Physique Fondamentale
59655 VILLENEUVE D'ASCQ (France)

Mr. J.M. MONGET
Centre de Télédétection et d'Analyse des milieux naturels
Ecole des Mines
Sophia-Antipolis
06560 VALBONNE (France)

Pr. F. VERGER
Laboratoire de Géographie
Ecole Normale Supérieure
1, rue Maurice Arnoux
92410 MONTROUGE (France)

SATELLITE DETERMINATION OF THE MESOSCALE VARIABILITY OF THE SEA-SURFACE TEMPERATURE

P.Y. DESCHAMPS [1], R. FROUIN [1], L. WALD [2]

(1) Laboratoire d'Optique Atmosphérique, Equipe associée au C.N.R.S., Université des Sciences et Techniques de Lille, 59655 Villeneuve d'Ascq Cédex, France.

(2) Centre de Télédétection et d'Analyse des Milieux Naturels, Ecole Nationale Supérieure des Mines de Paris, Sophia-Antipolis, 06560 Valbonne, France.

29 août 1980

ABSTRACT

Satellite infrared data have been used to investigate the mesoscale variability of the SST (Sea Surface Temperature) field. A statistical two-dimensional analysis of the SST field has been performed by means of the structure function. Results give the equivalent power law exponent, n, of the spatial variance density spectrum, $E(k) \sim k^{-n}$. n was found to vary from 1.5 to 2.3 with a mean value of 1.8 in the range of scales 3-100 km, in agreement with previous one-dimensional analysis from shipborne and airborne measurements. These observed values of n are discussed and compared to the values predicted by turbulence theories.

1. Introduction

The present capability of satellite infrared radiometers permits the determination of the mesoscale SST (Sea Surface Temperature) field on an operational basis thanks to their improved radiometric performances, which are typically a few tenths of (°C) for a nadir resolution of 1 km^2. This gives a potential tool for a systematic investigation of mesoscale thermal features such as thermal fronts and gradients which have already been detected and studied by means of infrared imageries or derived SST maps. Besides these observable features, a part of the SST field must be considered as random and containing some other information which can only be retrieved by a statistical analysis - e.g. the spectral density of variance.

Attempts to compute the spatial spectrum of the SST have been previously made by Mc Leish (1970), Saunders (1972 a) and Holladay and O'Brien (1975), from airborne infrared measurements along the aircraft track. Examples of mesoscale spectra have also been given from shipborne measurements (Voorhis and Perkins, 1966, Fieux et al., 1978), but more frequently for time series than for spatial variations. On the other hand, the satellite observations give the unique opportunity of investigating the mesoscale variability of the SST field, in the two-dimensions, down to scales of 1 km, at any given time, with a frequency which is limited only by the cloud cover. In this study, we intend to demonstrate the feasability of using satellite data to obtain statistical parameters of the mesoscale SST field.

2. Statistical analysis of the SST field

Studies of the variability of the temperature (or any scalar) field usually make an extensive use of spectral methods - i.e. the computation of the spectrum of the density of the scalar variance by means of Fourier transform or autocorrelation function , to obtain a typical power law which characterizes the variability of the temperature field and which can be referred to turbulence theories. In the present study, the structure function has been preferably used to determinate more accurately the power law exponent in the presence of the large noise level of satellite infrared data.

2.1 - Structure function

The SST field is considered as an isotropic random process with homogeneous increments (locally homogeneous) for which the structure function can be computed as :

$$D_{TT}(h) = \frac{1}{2} \; E \; \{T(x+h) - T(x)\}^2 \qquad (1)$$

where $T(x)$ = temperature at x,

h = scale, $k = h^{-1}$ = wavenumber,

E = average operator.

The main advantage of the structure function, $D(h)$ when compared to the spectrum of the variance density, $E(k)$, or the autocorrelation function, $B(h)$, is that the experimental determination of the structure function is more accurate and much less affected by random variations because only increments are taken into account (Panchev, 1971). An example is given in Fig. 1 where both $E_T(k)$ and $D_{TT}(h)$ have been computed and are shown for the same sample of the SST field, measured by the AVHRR (Advanced Very High Resolution Radiometer) experiment on board the TIROS-N satellite. This example shows clearly that the structure function is more regular than the spectrum, allowing an easier determination of the characteristic parameters - e.g. the power law exponent given by the slope when using logarithmic coordinates.

2.2 -Interpretation of the structure function

The structure function D(h) statistically represents the influence of a point upon the h-distant points. For an homogeneous and isotropic random process, D(h) and B(h) are linked by the following relationship :

$$D(h) = B(o) - B(h) \tag{2}$$

As B(h) and E(k) are the Fourier transform of each other, D(h) may thus be related to E(k) (Panchev, 1971) :

$$D(h) = 2 \int_o^\infty (1-J_o(kh))\ E(k)\ dk \quad \text{(2-dimension field)} \tag{3a}$$

$$D(h) = 4 \int_o^\infty (1 - \frac{\sin kh}{kh})\ E(k)\ dk \quad \text{(3-dimension field)} \tag{3b}$$

where $J_o(kh)$ is the zero order Bessel function of the first kind.

In geophysics, the spectrum is usually expressed in the following way :

$$E(k) = B\ k^{-n} \tag{4}$$

and then, from (3a), (3b), the structure function may be written as :

$$D(h) = A\ h^p \tag{5}$$

where A and B are constants,

n and p are exponents, which may be deduced from each other by :

$$n = p + 1 \quad . \tag{6}$$

so that the exponent, n, of the spectrum can be altarnately determined from the structure function, using (6), as far as the field under study is homogeneous.

Two kinds of error may affect the determination of the SST field obtained from satellite : instrumental data noise, atmospheric effect.

Although the structure function has the advantage of being much more regular than the spectrum, the study of the structure function and of its shape is generally limited by the noise level at the smallest scales. This effect is illustrated in Fig. 1b, where the observed slope giving the power law exponent of the structure function decreases from about 1 at larger scales, to 0 at smaller scales. This is due to the fact that the structure function of the instrumental noise adds to the SST one . As far as this noise is white, its structure function is a constant (p=o) and its addition restricts the statistical analysis at smaller scales. This effect can be reduced by spatial smoothing with a corresponding degradation of the ground resolution.

Smoothing also introduces a bias in the determination of the structure function. If $D_F(h)$ is the structure function of the smoothed field, and Q is the convolution square of the smoothing function F, it may be shown (Matheron, 1970) that :

$$D_F(h) = D * Q - A \tag{7}$$

10

where $*$ means convolution and A is a constant.:

$$A = \int_{-\infty}^{+\infty} D(u)\ Q(u)\ du \qquad (8)$$

In the particular case where F is the spatial average in a square and where the structure function $D(h) \sim h^p$, with $0.5<p<1.5$, the influence of smoothing on the amplitude of the structure function D(h) increases with p, but decreases rapidly when h increases, and is less than 10 % when h is equal to 5 times the dimension of the smoothing square. The influence of spatial smoothing was thus neglected in the present study.

As far as the variations of the atmosphere can be neglected within the mesoscale oceanic range, the observed satellite variations of the SST field are reduced by the atmospheric infrared transmittance, τ (Deschamps and Phulpin, 1980) :

$$T(x+h) - T(x) = \tau(T_s(x+h) - T_s(x)) \qquad (9)$$

where T_s is the actual SST,

T is the measured SST from space.

Then :

$$D_{TT}(h) = \tau^2\ D^s_{TT}(h) \qquad (10)$$

where D^s_{TT} is the actual structure function. τ depends on the atmospheric water vapor content and ranges between typical values of 0.9 to 0.3 for the 10.5 - 12.5 µm channel mostly used on satellites. This atmospheric effect will affect the determination of the amplitude of the structure function, but not the determination of the power law exponent, p. Because the atmospheric transmittance cannot be accurately determined over the oceans, only one parameter of the structure function can be determined from satellite, and this is the power law exponent, p, obtained from the slope of the curve in a log-log plot.

The hypothesis of the homogeneity of the random field must be verified, otherwise erroneous determinations of the exponent could be obtained. For example, a frontal zone would have a spectrum $E_T(k) \sim k^{-2}$ and a structure function $D_{TT}(h) \sim h$, while a non-removed trend would also give $E_T(k) \sim k^{-2}$, but $D_{TT}(h) \sim k^2$. Because these exponents are close to the values physically expected, it is necessary to check carefully the homogeneity of the SST field and to remove the existing trend when necessary.

3. Results

The results of two independent but complementary studies are hereby presented. The first one deals with data obtained from the VHRR (Very High Resolution Radiometer) on board NOAA-5 and the study was limited to the range of scales 40-100 km because of the large level of instrumental noise. The improved radiometric performances of the HCMM (Heat Capacity Mapping Mission) data, - i.e. a nadir resolution of 0.5 km and NEDT = 0.3° K(see Table 1) - allowed us to extend the study down to scales of 3 km.

Cloudfree satellite data were selected in homogeneous study areas, Northeastern Atlantic Ocean and Mediterranean Sea. Locations are shown in Fig. 2 and dates are given in Table 2. At each one of these locations, the unidimensional structure functions were computed in four directions, $\Theta = 0$ (across the satellite track - i.e. approximatly east to west), $\pi/4$, $\pi/2$ (along the satellite track) and $3\pi/4$. More details on the processing of the data may be found in Frouin (1980) and Wald (1980). Examples of the computed structure functions are given in Fig. 3 for VHRR/NOAA-5 and in Fig. 4 for HCMM. The results generally show that the SST field is not exactly isotropic. Nevertheless, the structure functions, if not equal, are roughly parallel on a log-log plot, so that the anisotropy is confined in the amplitude, $A(\Theta)$:

$$D_{TT}(\Theta,h) = A(\Theta)\ h^{p} \tag{11}$$

but the slope p remains very isotropic.

Values of p from 0.5 to 1.3 have been observed in this study with an estimated accuracy of about 0.1. Using VHRR/NOAA-5 data, 44 estimations of p were made in the range of scales 40-100 km, and 37 estimations in the range of scales 3-30 km with HCMM data. The corresponding histograms of the observed p are given in Fig.5a and Fig.5b. The most frequent values are 0.9-1.0 and the mean values are 0.8 (3-30 km) and 0.9 (40-100 km) with a standard deviation of about 0.2. About 90 % of the observed values are distributed between 0.5 and 1.1. The results correspond to a mean value of the power law exponent of the spectrum, n, of 1.8 in the wavenumber range 0.01-0.3 km^{-1}.

The amplitude of the structure functions varied from 10^{-2} to 10^{-1} $(°C)^2$ at h = 40 km. Even after spatial smoothing, it was noted that the noise level had a slight tendancy of reducing the estimated of values of p because the structure function of the noise is a constant (p=o). This is particularly effective when the noise level (5.10^{-3} $(°C)^2$ for the HCMM data, 3.10^{-2} $(°C)^2$ for the VHRR/NOAA-5 after smoothings) is of the same order as the structure function (see Fig. 1). Whenever possible, the estimates of p were corrected for this effect, but the effect could partly explain the lowest values of p.

On the other hand, a mean horizontal thermal gradient would give $D(h) \sim h^2$. The areas studied were carefully selected to avoid the existence of such thermal gradients which would increase the estimate of p towards larger values ; but here again some influence on the data could remain. Both these two effects, noise level and horizontal thermal gradients, could partly but not totally explain the spread of the results around the mean value, between 0.5 and 1.3, which remains significant. There is no evidence of correlation between the estimates of p and the corresponding geographical locations or seasons, but nevertheless, we would guess that it is probably necessary to involve physical processes in the explanation of the observed p values.

4. Discussion

Using Eq. 6 and the result from this structure function analysis, we obtain $1.5<n<2.3$ for the power exponent of the spectrum. This agrees fairly well with the previous results reported by several authors either from shipborne measurements (Fieux et al, 1978), or from airborne infrared measurements (Saunders, 1972a), for the one-dimensional temperature spectra (see Table 3). Holladay and O'Brien (1975) also made an attempt to reconstruct the two dimensional SST field from the tracks of the aircraft survey and found $n \simeq 3$ for the isotropic part of the two-dimensional spectrum, a value which is probably overestimated because of the smoothing of high wavenumbers produced by the SST mapping procedure.

It would be interesting to relate the computed values of n to those given by turbulence theories in geophysics. All these theories assume the existence of an inertial range, i.e. the considered scales ~~are~~ far from the energy sink and source scales. It is not evident that the range of scales 3-100 km in the ocean is an inertial one. The upper limit of the dissipation scale is of the order of 500 m and can be related to the wavelength of surface and internal waves via breaking processes. This scale is about one decade smaller than the lower limit of the studied range and we consider that there is no interaction between these two scales. The scales of imput of kinetic energy and of temperature variance remain puzzling. Input of kinetic energy related to the wind is found at scales of the order of the wind waves (100 m) and at scales of the meteorological systems (1000 km or more). Energy inflow due to thermodynamic forcing is found at even larger scales. All these scales are one or two order of magnitude smaller or greater than those studied. At some location, interior processes such as baroclinic eddies or baroclinic instability may also play an important role in converting energy through non-linear mechanisms. The scales of these phenomena are of the same order as the internal radius of deformation or two to six times greater, depending on initial conditions. This radius is of about 50 km in the open ocean and 10 km in the Mediterranean sea. If these physical processes are of importance in the area studied, the range 3-100 km is not an inertial one. In fact, we cannot precisely determine this from our observations : by looking at Fig. 3 and 4, one can notice that the structure functions do not exhibit any peak characterizing a very energetic scale in the range we deal with, but this may only mean that the energy inputs are outside the studied range.

In the range of scales 3-100 km, horizontal scales are larger compared to vertical ones and the observed variability may be considered as being a quasi two-dimensional process. Therefore the observations can be related to the n-values predicted by the theories of bidimensional turbulence (Kraichnan, 1971) and of geostrophic turbulence in the atmosphere (Charney, 1971). These theories take into account either the conservation of energy and the conservation of enstrophy (half of the mean square of the vorticity) in the case of Kraichnan's theory or the pseudo-potential enstrophy (Charney). Both these theories agree when predicting the power law of the kinetic energy spectrum : $E_K(k) \sim k^{-3}$.

But the relations between current and temperature are not obvious and the different mechanisms involved lead to drastically different theoretical power laws for the temperature variance spectrum. In Kraichnan's theory, considering that temperature is a passive contaminant implies that $E_T(k)$ only depends upon k and upon the dissipation rates of enstrophy and temperature variance. Then, from a dimensional analysis, $E_T(k)$ must follow a k^{-1} power law. Charney made use of the perfect gas law and of the hydrostatic relation to compute a relation between the temperature and the stream function and he found the same law for $E_T(k)$ as for $E_K(k)$ - i.e $E_T(k) \sim E_K(k) \sim k^{-3}$. Furthermore, assuming also $E_K(k) \sim k^{-3}$, Saunders (1972b) exhibited a temperature variance spectrum $E_T(k) \sim k^{-5}$, by the use of the thermal wind equation. These examples show that the results may be very different according to various authors. In this study, the mean observed value of 1.8 for n is far from the assessment (n=5) made by Saunders but falls between the Kraichnan and Charney predictions (n=1 and 3). This discrepancy may be due to the fact that the theories hypothesises have not been respected, in particular the hypothesis that the range studied is not an inertial one.

Some three-dimensional theories of turbulence (Kolmogorov, 1941, Bolgiano, 1962) or space-time variability theories of internal waves (Garrett and Munk, 1972, 1975) report values of n close to those found in our study (respectively 1.7, 1.4 and 2), but their physical basic hypothesis can hardly be extended in the mesoscale range.

We may also notice that several studies of atmospheric temperature fields mention values of n in agreement with our study at similar range of scales (100-1000 km). One may refer to the reviews by Gage (1979) and Panchev (1971). Some of these results are obtained by using spectral analysis on time-series data and equivalent wavenumbers are computed by using Taylor's relation. As the validity of this relation is dubious for such scales, these time-series results must be considered carefully. But as for the oceanographic observations, there is no atmospheric theory to explain the observed results.

In summary, the power law exponent n of the spectral temperature variance observed in the range of scales 3-100 km is nearly 2. A large discrepancy exists with the predicted values from the 2 - dimensional turbulence theories which are widely spread around this value, and we need further advanced theories to explain the experimental determination of the mesoscale SST variability.

5. Conclusion

In this study, it has been proved feasible to estimate the random properties of the SST field in the mesoscale range 3-100 km from satellite infrared data. Compared to previous 1-dimension analysis from shipborne and airborne observations, the use of satellite data allowed us to perform a 2 - dimensional analysis. Using the structure function, the power law exponent, n, of the spectrum of the variance density of the SST field can be retrieved within a good accuracy ($\pm$ 0.1). A mean value of 1.8 and a standard deviation of 0.2 have been found in the range 3-100 km, and extreme values of 1.5 and 2.3 have been observed.

The results give rise to several questions : (i) Is the range 3-100 km an inertial one ? (ii) If yes, is there any turbulence theory to explain the spectrum power law observed ? (iii) If not, at which scales are the inputs of energy and to which processes are they related ? At the present time, further investigations, both theoretical and experimental, are needed to interpretate the physical mechanisms and parameters involved in the mesoscale variability of the SST field.

ACKNOWLEDGEMENTS

The authors are indebted to the receiving station of the "Meteorologie Nationale" at Lannion, France, for providing them the infrared data from meteorological satellites. HCMM data have been received from NASA as a support to HCMM investigation number 15. They wish also to acknowledge the helpful advices of J.M. Monget and the fruitful suggestions of M. Crepon. Supports for this work have been provided by the following french agencies : CNRS (Centre National de la Recherche Scientifique), CNES (Centre National d'Etudes Spatiales) and CNEXO (Centre National pour l'Exploitation des Océans).

REFERENCES

BOLGIANO, R., 1962 : Structure of turbulence in stratified media. J. Geophys. Res., 67, 8, 3015-3023.

CHARNEY J.G., 1971:Geostrophic turbulence. J. Atmos. Sci., 28, 1087-1095.

DESCHAMPS, P.Y. and T. PHULPIN, 1980 : Atmospheric correction of infrared measurements of sea surface temperature using channels at 3.7, 11 and 12 µm. Boundary-Layer Meteorol., 18, 131-143.

FIEUX, M., S. GARZOLI and J. GONELLA, 1978 : Contribution à la connaissance de la structure spatiale des courants superficiels au large du golfe du Lion. J. Rech. Oceanogr., 3,4.

FROUIN, R., 1980 : Contribution apportée par l'expérience spatiale HCMM à la télédétection de la température de surface de la mer. Thèse de 3e cycle, Université de Lille I.

GAGE, K.S., 1979 : Evidence for a $k^{-5/3}$ law inertial range in mesoscale two dimensional turbulence. J. Atmos. Sci., 36, 1950-1954.

GARRETT, C. and W. MUNK, 1972 : Space time scales of internal waves. Geophys. Fluid Dynamics, 3, 225-264.

GARRETT, C. and W. MUNK, 1975 : Space time of internal waves : a progress report. J. Geophys. Res., 80, 3, 291-297.

HOLLADAY, C.G. and J.J. O'BRIEN, 1975 : Mesoscale variability of sea surface temperature. J. Phys. Oceanogr., 5, 761-772.

KOLMOGOROV, A.N., 1941 : The local structure of turbulence in incompressible viscous fluid for very large Reynolds numbers. Dokl. Akad. Nauk. SSSR, 30, 301-305.

KRAICHNAN, R.H., 1971 : Inertial-range transfer in two-and three-dimensional turbulence. J. Fluid Mech., 47,3, 525-535.

KRAICHNAN R.H., 1974 : Convection of a passive scalar by a quasi-uniform random straining field. J. Fluid Mech., 64, 4, 737-762.

Mc LEISH, W., 1970 : Spatial spectra of ocean surface temperature. J. Geophys. Res. 75, 6872-6877.

MATHERON G., 1970 : La théorie des variables régionalisées et ses applications. Cahiers du Centre de Morphologie Mathématiques de Fontainebleau. Ecole des Mines de Paris, Editors.

PANCHEV, S., 1971 : Random functions and turbulence. Pergamon Press, 444 p.

SAUNDERS, P.M., 1972 a : Space and time variability of temperature in the upper ocean. Deep-Sea Res., 19, 467-480.

SAUNDERS, P.M., 1972 b : Comments on "Wavenumber-frequency spectra of temperature in the free atmosphere". J. Atmos. Sci., 29, 197-199.

VOORHIS, A.D. and PERKINS H.T., 1966 : The spatial spectrum of short-wave fluctuations in the near surface thermocline . Deep-Sea Res., 13, 641-654.

WALD, L., 1980 : Utilisation du satellite NOAA-5 à la connaissance de la dynamique océanique. Etude de ses variations saisonnières en Mer Ligure et de ses variations spatiales en Méditerranée. Thèse de 3e cycle, Université de Paris VI.

Table 1. Radiometer performances of the satellite experiments used in this study.

Satellite experiment	Ground resolution at nadir (km)^2	Noise equivalent temperature difference (°C)
VHRR/NOAA-5	1	0.8
HCMR/HCMM	0.25	0.3
AVHRR/TIROS-N	1	0.1

Table 2. Summary of the different areas studied

Area	Date	Location	Experiment
Eastern Mediterranean Sea	19 Mar.,1978	33°00'N-28°00'E	VHRR
"	05 May ,1978	34°00'N-15°00'E	"
"	08 May ,1978	33°00'N-29°00'E	"
"	14 May ,1978	33°30'N-28°30'E	"
"	17 May ,1978	33°30'N-26°00'E	"
Western Mediterranean Sea	29 Sep.,1977	41°00'N-04°00'E	"
"	29 May ,1978	39°05'N-07°15'E	HCMM
"	29 May ,1978	40°05'N-06°55'E	"
"	11 Jul.,1978	38°55'N-04°50'E	"
"	11 Jul.,1978	41°55'N-06°55'E	"
"	26 Jul.,1978	39°20'N-06°15'E	"
"	28 Jul.,1978	38°15'N-03°45'E	"
"	28 Jul.,1978	38°35'N-05°05'E	"
"	28 Jul.,1978	37°40'N-07°25'E	"
"	14 Aug.,1978	38°30'N-03°00'E	VHRR
"	14 Sep.,1978	40°25'N-06°30'E	HCMM
"	1[illegible] Sep.,1978	40°35'N-11°55'E	"
"	14 Sep.,1978	41°40'N-06°45'E	"
Northeastern Atlantic Ocean	11 Sep.,1977	46°00'N-06°30'W	VHRR
"	14 Sep.,1977	45°00'N-07°00'W	"
"	06 Jan.,1978	46°30'N-09°00'W	"
"	10 May ,1978	46°00'N-08°00'W	"
"	11 May ,1978	45°15'N-04°40'W	HCMM
"	11 May ,1978	38°35'N-11°45'W	"
"	18 Jun.,1978	46°00'N-08°35'W	"

Table 3. Summary of observed mesoscale SST variability.

Authors	Range of scales (km)	Power law exponent n	Comments
SAUNDERS (1972)	3 - 100	2.2 ± 0.1	1-D,surface temperature,airborne infrared sensor.
HOLLADAY and O'BRIEN (1975)	3 - 20	3	2-D,SST maps from aircraft surveys.
FIEUX and Al. (1978)	1 - 64	2	1-D,surface temperature,ship-towed sensors.
This study	3 - 100	$1.5 < n < 2.3$; $\bar{n} = 1.8$	2-D,surface temperature,satellite data.

CAPTIONS

Figure 1 - Comparison between the density of temperature variance $E_T(k)$ (a) and the structure function $D_{TT}(h)$ (b), computed from AVHRR data, July 17, 1979, over the Bay of Biscay (45° 30' N - 4° 30' W). The dashed line indicates the radiometer noise level.

Figure 2 - Geographical locations of the different study areas for HCMM data (▼), and VHRR data (●).

Figure 3 - Example of structure functions computed from VHRR data.

Figure 4 - Example of structure functions computed from HCMM data.

Figure 5 - Histograms of the observed values of the power law exponent p of the structure function in the range of scales 40 - 100 km (a) and in the range of scales 3-30 km (b).

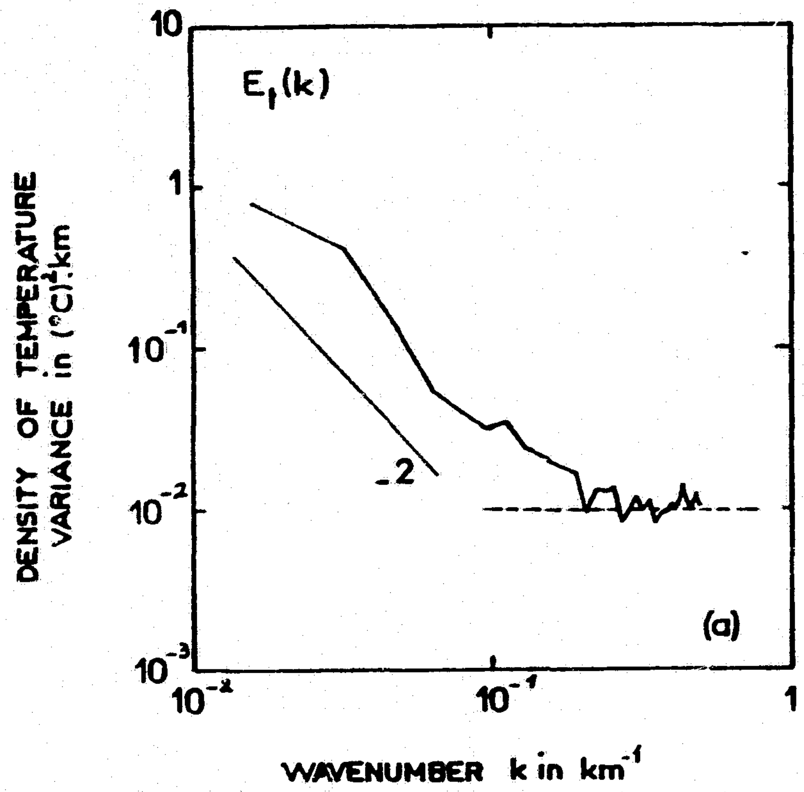

Fig. 1a

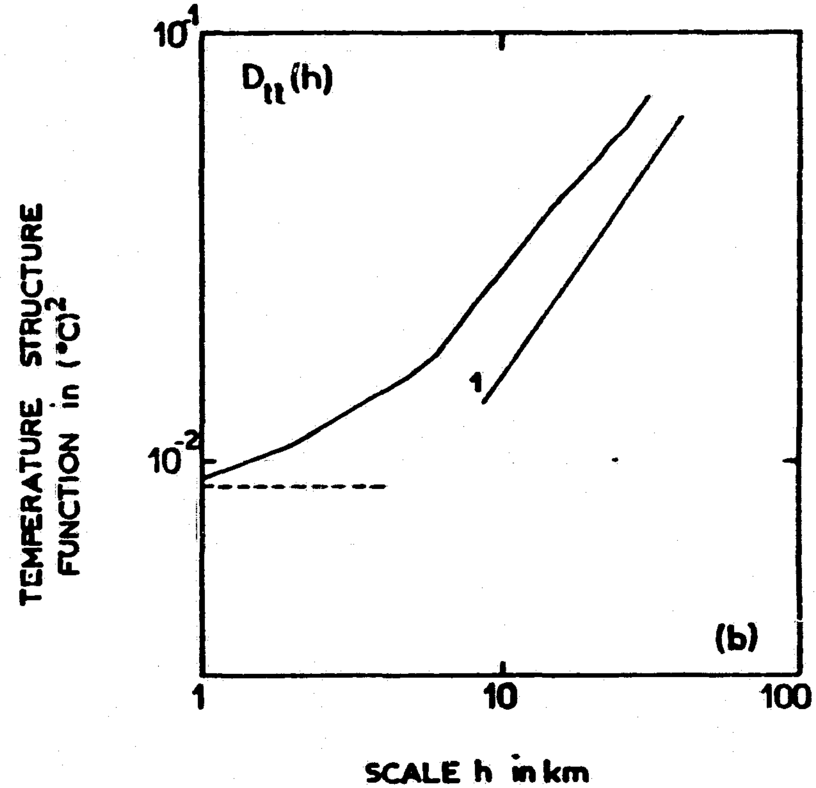

Fig.1b

Figure 1 – Comparison between the density of temperature variance $E_t(k)$ (a) and the structure function $D_{tt}(h)$ (b), computed from AVHRR data, July 17, 1979, over the Bay of Biscay (45° 30' N – 4° 30' W). The dashed line indicates the radiometer noise level.

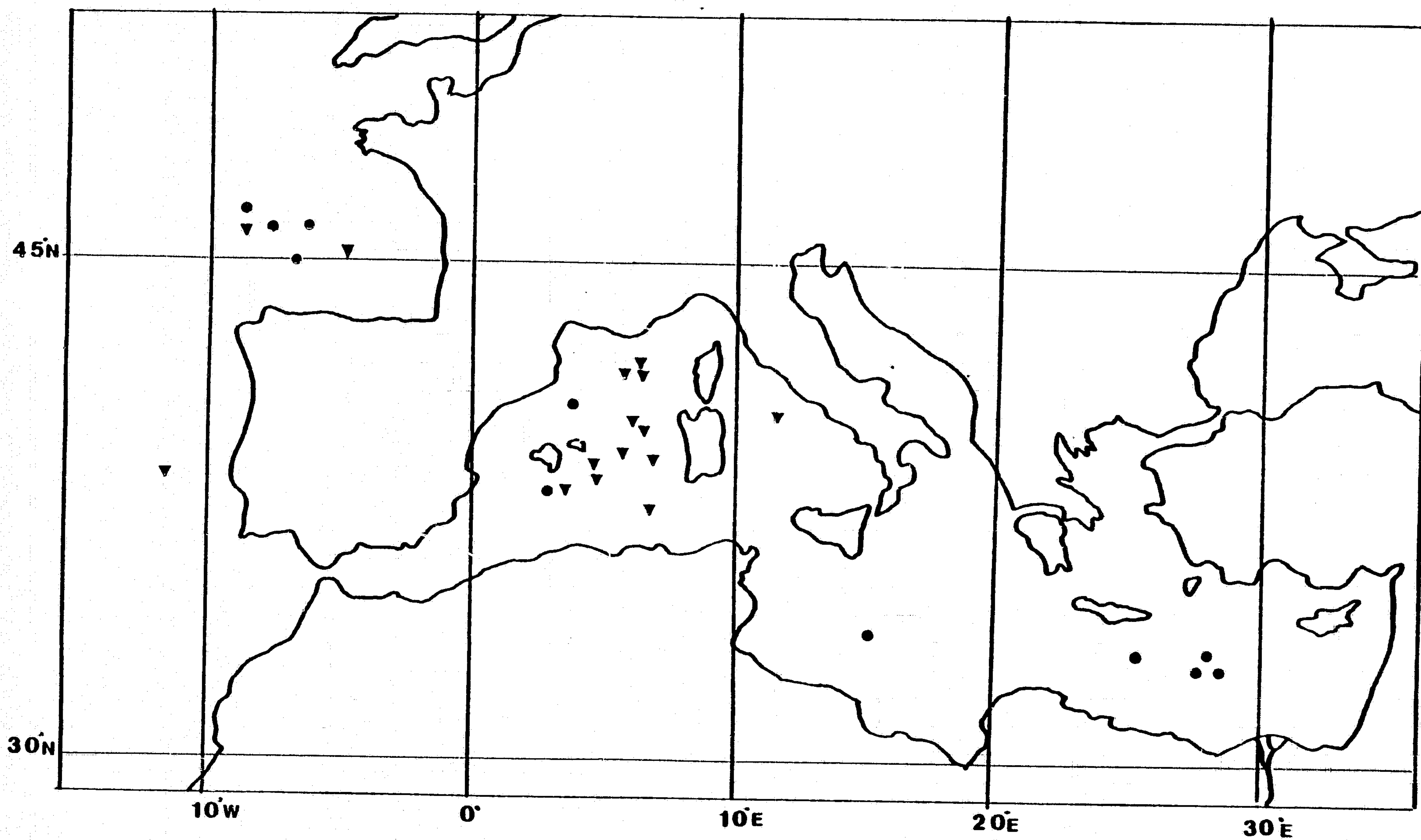

Fig. 2

Figure 2 - Geographical locations of the different study areas for HCMM data (▼), and VHRR data (●).

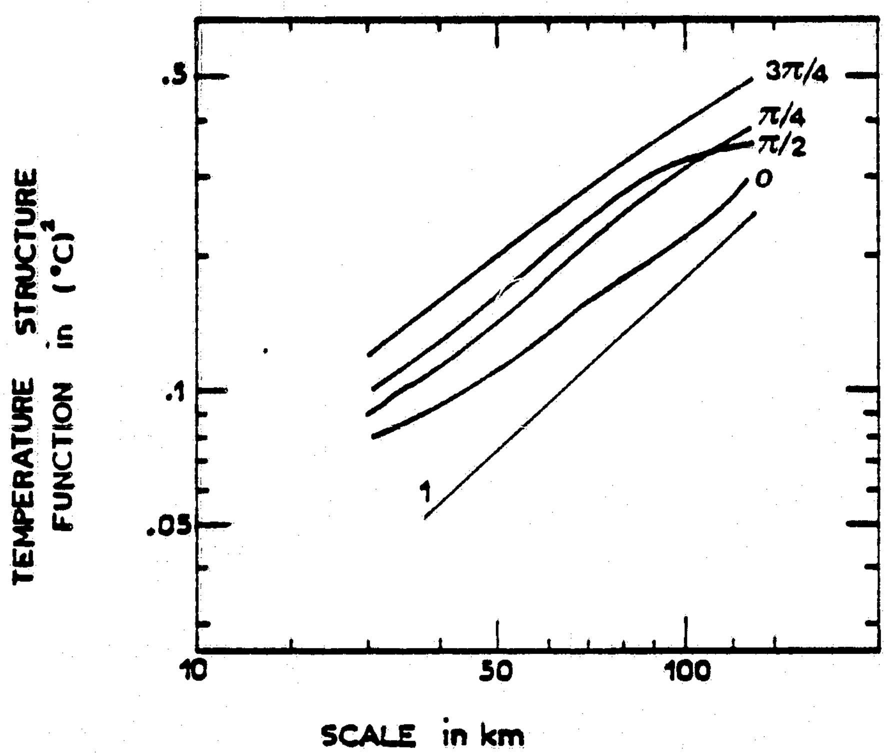

Fig. 3

Figure 3 - Example of structure functions computed from VHRR data.

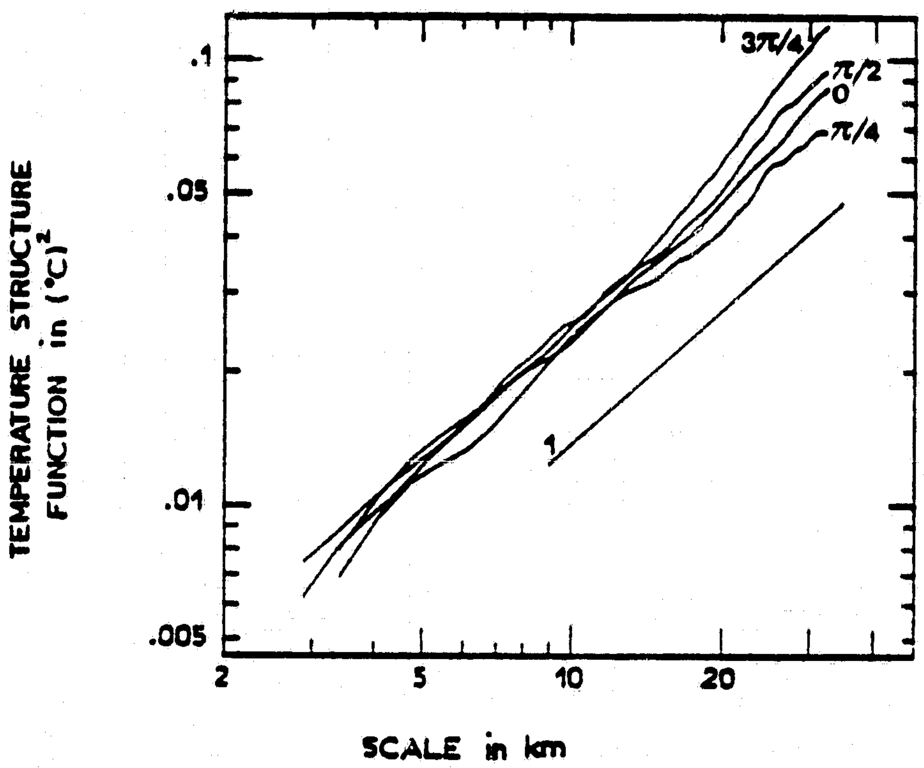

Fig. 4

Figure 4 - Example of structure functions computed from HCMM data.

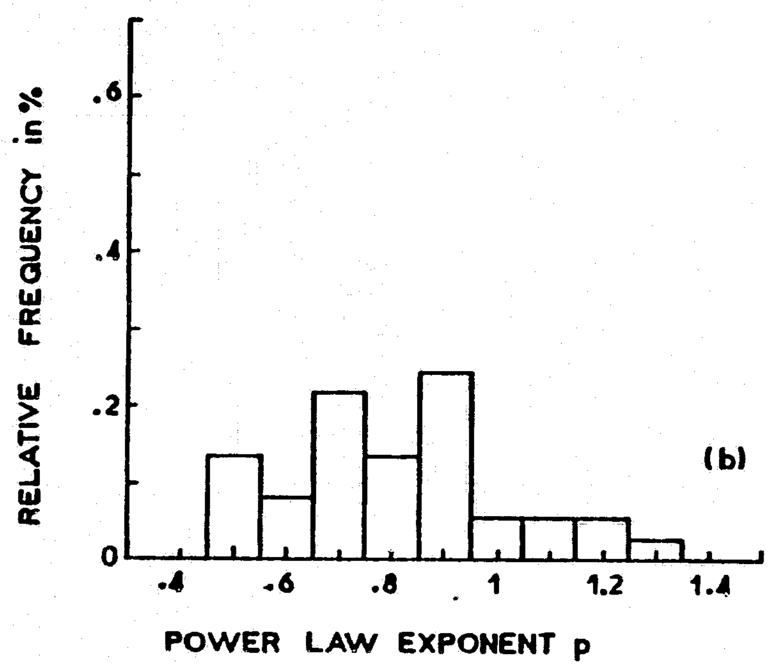

Fig. 5b

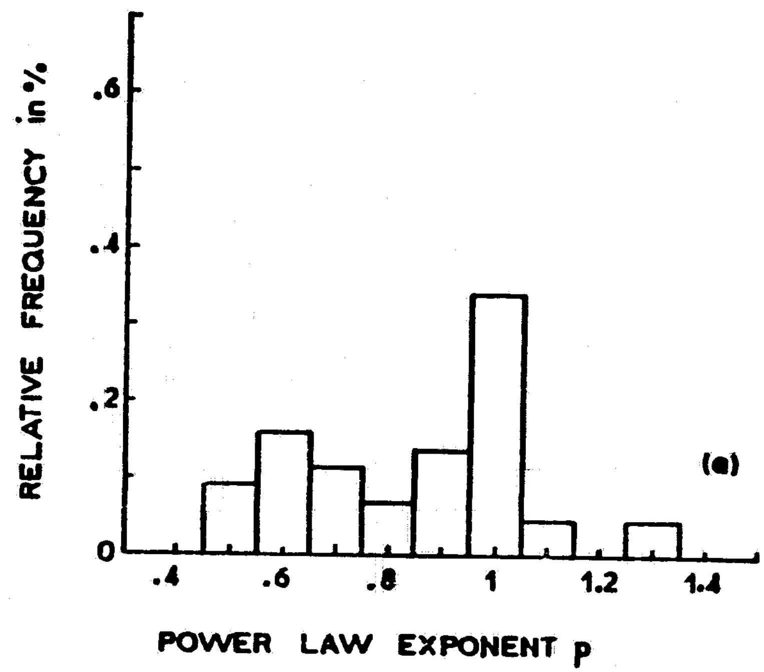

Fig. 5a

Figure 5 - Histograms of the observed values of the power law exponent p of the structure function in the range of scales 40 - 100 km (a) and in the range of scales 3-30 km (b).

LARGE DIURNAL HEATING OF THE SEA SURFACE OBSERVED BY THE HCMM EXPERIEMENT

P.Y. DESCHAMPS AND R. FROUIN

Laboratoire d'Optique Atmosphérique,

Equipe Associée au CNRS n° 466,

Université des Sciences et Techniques de Lille,

59655 Villeneuve d'Ascq Cédex, France

ABSTRACT

Day-night surface temperature differences have been measured in the infrared (10.5 - 12.5 μm channel) by the HCMM satellite experiment, which show large diurnal heating (several °C) of the upper layer of the ocean, very frequently during summer months in the Mediterranean Sea, when the wind speed is low. When observed in the 0.5 - 1.1 μm channel, glitter reflectance - i.e. direct solar radiation specularly reflected towards the sensor - correlates whith diurnal heating. Glitter reflectance has been modelized to retrieve an equivalent wind speed , and observed diurnal heatings, ΔT, rapidly decrease with the wind speed, U, from a maximum value of about 5° C. An empirical law is given : $\Delta T_{(°K)} \simeq 3.5.10^{-3}\ Q_{(W.m^{-2})} / (0.7 + U_{(M.s^{-1})})$ where Q is the irradiance at sea level. A mean diurnal heating of nearly 1° C is calculated for the marine coastal areas of the south France, in summer time. During this period, satellite observations should be restricted to night and early morning times, and to the only high wind speed ($U > 5\ m.s^{-1}$) at noon and during the afternoon.

31

I - INTRODUCTION

A daily variation of the temperature in the surface layer of the oceans is known to be produced by the diurnal heating of the absorbed solar radiation. The amplitude of the daily temperature is usually small because of the large turbulent mixing which usually prevails over the molecular thermal diffusivity. A solar irradiance of 1000 $W.m^{-2}$ when absorbed in a mixed layer of 10 m would only give a heating rate of 0.1° C per hour, and a daily variation of less than 0.5° C. While if the turbulent mixing is reduced and the mixed layer thickness is restricted to less than 1 m, a heating rate of 1° C per hour may be expected and daily variations of several °C should be observed. With the exception of very shallow waters, large diurnal heatings in open oceans thus correspond to the case of lower wind speeds as far as turbulence in the upper surface layer is mostly locally in-duced by the surface wind stress.

From a theoretical simulation of radiative and heat transfer in the upper ocean layer, HASSE (1971) has pr~~e~~dicted that the deviation of the sea surface temperature (SST) T_o from the bulk temperature T_{10} taken at 10 meter-depth should vary as :

$$T_o - T_{10} = C_2 \, Q \, U^{-1} \tag{1}$$

where Q is the solar irradiance, U, the wind speed, and $C_2 = 3.5\ 10^{-3}$ when Q is expressed in $W.m^{-2}$, U in $m.s^{-1}$. According to HASSE, Eq.(1) is only valid for $U \geq 2 m.s^{-1}$, but the evidence that the SST diurnal variations increases when U decreases is supported by several observations : ROMER (1969), STOMMEL et al (1970) where large diurnal variations of more than 1° C are occasionaly found at very low wind speeds - i.e. for $U < 2 m.s^{-1}$. These observations are nethertheless restricted to a single location and limited time occasions.

Satellite infrared radiometers offer the opportunity to investigate more systematically such large diurnal variations of the SST. The first satellite experiment to provide adequate capability for this purpose was the HCMR (Heat Capacity Mapping Radiometer) experiment launched in late April 78 with an improved temperature resolution (0.3° C) and a nearly noon overpass. Results from this experiment are hereby reported in order (i) to investigate large diurnal SST variations at low wind speeds (ii) to give an assessment of the relation frequency of such an event and its impact on the determination of the SST field in such area ~~ak~~ like Mediterranean Sea where the occurence of diurnal heating is rather large.

II - OBSERVATIONS OF DIURNAL HEATING FROM HCMR SATELLITE DATA

II-1 - The HCMR experiment

The basic objectives of the HCMR experiment are to measure diurnal variations of the earth surface temperature for applications to earth resources (geology, hydrology...). For this purpose, the satellite is sun-synchronous and its orbit was chosen to cross the equator at about 2 a.m and 2 p.m local time so that surface temperature data are obtained close to the minimum and the maximum of the diurnal variation. Satellite altitude is 620 km, and orbit inclinaison is 98.87° . The HCMR consists of a two-channel scanning radiometer, with a 0.5 - 1.1 µm spectral bandwith in the visible and 10.5 - 12.5 µm in the thermal infrared. Similar channels have been used on previous meteorological satellites, but the interests of the HCMR experiment are (i) a large improvment of the radiometric performances in the thermal infrared channel for which the temperature resolution is 0.3° C and the nadir ground resolution is 500 m as compared to respectively 0.7° C and 1 km for the previous VHRR/NOAA satellite, (ii) the facility offered to the user to obtain differential surface temperature maps between day and night at 12 or 36 hours intervals. The HCMR experiment was originally designed to produce thermal inertia data for soil and geology applications but the very good performances of HCMR are suitable also for oceanographic studies. Data were received from NASA (National Administration for Space Research) through an investigation concerned with sea surface temperatures of the coastal zones of France.

Available HCMR data are photographic or digital products covering a 700 x 700 km^2 square scene. The following informations are displayed : (1) surface diffuse albedo or reflectance in the visible channel (day only), (2) surface temperature from the infrared channel, (3) surface temperature difference between day and night, (4) thermal inertia, which was not used in the present study. About 1000 scenes covering the coastal zones of France were received for the period May 1978 - May 1979. Examples of the photographic products are given for two areas in the Western Mediterranean Sea (Fig. 1) and in the North Sea (Fig. 2)) where large diurnal variations of the SST were observed.

II-2 - Diurnal heating and glitter (sun glint) patterns

A large number of the received data from May to July 1978, over the Mediterranean Sea exhibited very interesting and similar features in both the visible and the infrared channels, as shown in Fig. 2. between Corsica Island and the south coast of France, and also close to the east coasts of of Corsica and Sardinia Islands.

Warmer areas in the thermal channel are associated with changes of brightness in the visible.

The observed changes of brightness in the visible are identified as glitter or sunglint patterns - i.e. specular reflexion of direct solar radiation by the wavy sea surface. During the concerned period around the summer solstice, the observation angle of the HCMR imagery was allowed to be very close to the specular reflection of direct solar radiation, in the western part of the scenes, which is favorable for observations of glitter patterns. Most of the time, the glitter increases from rough to calm seas, when the wind decreases and the sea surface becomes more specular, and exhibits a maximum brightness when the observation angle is close to the specular reflexion of solar radiation : a homogeneous bright area is thus noted in the south-west part of Fig. ~~2a~~ 1-a. But for very calm seas, the surface reflexion becomes nearly specular, and a decrease of the brightness may also be observed because it is very unlikely that the observation angle is strictly towards the specular reflexion. Such a darkening is observed in the northwest part of Fig. ~~2a~~ 1a, where the two processes are present with both bright and dark areas corresponding respectively to weak and nul wind speeds. The fact that smoothing of the surface could produce either an increase or a decrease of the glitter brightness was previously mentionned by LA VIOLETTE ~~and [illegible]~~ et al. (1980). A physical and detailed description is given in Appendix, to support a further quantitative analysis of the data. The dark patterns in a mean bright glitter can thus be clearly interpreted as nul wind and calm sea areas, which obviously are favourable to a larger diurnal heating of the upper layer of the ocean because the heat transfer to deeper ocean layers is limited by a low turbulent mixing and thermal diffusivity.

II-3 - Meteorological observations

Evidence of a large diurnal heating corresponding to low wind speed conditions is also given by correlative meteorological observations. Surface observations are presented in Fig. 1-d for the case in the Mediterranean Sea, and in Fig. 2-c for an other case found in the North Sea where, due to higher latitudes, glitter is almost always unobservable. On Fig. 2-a a large warm spot was detected by HCMR in the middle of the North Sea which is coincident with the center of high anticyclonic situation pressure when nul wind speed is reported. Warmer areas observed in the Mediterranean Sea on Fig. 1-b are also coincident with low or nul wind speeds, but the observed wind field is much more complicated because most of the reporting coastal weather stations are affected by some breeze effects wich surimpose to an anticyclonic circulation. Cloudfree satellite SST observations are frequently acquired during similar anticyclonic situations with moderate wind speeds. It must be outtined that satellite estimations of SST may thus be systematically affected by diurnal heating, and a tentative statement of this is discussed in section III-4.

II-4 - Day-Night observations

Heat loss during the night very rapidly destroys most of the diurnal heating, at least in the upper layer, which was produced during day time. Evidence of a diurnal heating may thus be found from a comparative analysis of two successive day and night observations at 12 hours intervals. For the two cases given in Fig. 1-c and 2-b, nightime observations show a much more constant SST field and the noticeable daytime warmer features disappear.

Figure 1-d gives the result of the computed day-night temperature differences after the proper calibration algorithms have been applied by NASA ______________ . These differences present the advantage to be independent of the mean mesoscale SST field and allow to enhance the diurnal heating, which again closely correlate with glitter patterns in the visible channel. Day-night temperature differences are used in the followings for a more quantitative analysis of diurnal heating.

III - DEPENDENCE OF DIURNAL HEATING ON SEA STATE AND WIND SPEED

The observed diurnal heatings were further quantitatively analysed to derive its relationship with the sea state and the wind speed. Day-night temperature difference were correlated to the reflectance of the 0.5 - 1.1 μm channel. This reflectance, mostly due to sun glitter, is related to the surface slope variance and to a mean wind speed using the statistical model from COX and MUNK (1955).

III-1 - Diurnal heating and glitter reflectance

Day-night temperature differences (Fig. 1-d) - i.e SST diurnal variations - show patterns similar to the glitter patterns (Fig. 1-a), on June 3, 1978. Fig. 3 gives the result of the correlation obtained when the diurnal heating, ΔT, is plotted as function of the glitter reflectance, ρ_g , in a small study area, east of Sardinia. Most evidently a close correlation exists and ΔT rapidly decreases when ρ_g increases. To further interpret that fact, ρ_g has to be related to the wind speed, or more exactly to the statistics of surface slopes.

Using the statistical distribution of surface slopes from COX and MUNK (1955), a model was developped to relate the glitter reflectance to the wind speed. This model is detailed in Appendix. Results indicate that ρ_g could either increase or decrease with wind speed : ρ_g presents a maximum value for a given wind speed value which both of them depend on solar and observation angles through Θ_n (tg Θ_n is the surface slope allowing specular reflection toward the sensor). Fig. 4 give the relationship between ρg and the wind speed, U, for $\Theta_n = 8°$, 10°, and 12°, which correspond to the area previously studied for $\Delta T = f(\rho_g)$. In this case ρ_g increases rapidly at the lower wind speeds and then is rather constant for $U > 3\ m.s^{-1}$ so that U can be estimated with a good accuracy from ρ_g, only for $U < 3\ m.s^{-1}$. The study has thus to be limited to this wind speed range. It should also be noted that ρ_g is physically linked to the surface slope variance, and only statistically to the wind speed. Local anomalies may thus occur, in particular when the fetch of the wind over the sea is variable. Keeping in mind these cautions, we may now transform $\Delta T(\rho_g)$ in $\Delta T(U)$ which is given in Fig. 5.

III-2 - Diurnal heating and the wind speed

The first point to be noted on Fig. 5 which gives the diurnal heating as a function of the wind speed, is that ΔT rapidly decreases from several °C to 1° C when U increases up to $2\ m.s^{-1}$. The scatter of observations on Fig. 5 is remarkably less than on Fig. 3 for $\Delta T(\rho_g)$, because the variations of ρ_g with changes of observation angles within the study area have been eliminated. A fit of $\Delta T(U)$ on Fig. 5 would give :

$$\Delta T = 0.4\ U + 1.1 \qquad (2)$$

(in °C for U in $m.s^{-1}$)

Some uncertainties related to the model $\rho_g(U)$ have been previously outlined. Additional errors may be due to atmospheric effects on the measured radiances. An aerosol atmospheric reflectance of about 0.02 was estimated from the minimum reflectance within the scene ($\rho_g \simeq 0$) and substracted in the 0.5 - 1.1 µm channel. Day-night temperature differences have not been corrected for atmospheric emission in the infrared. This approximation would be valid only if the atmosphere remains the same between the two satellite overpasses, but a bias due to a change of atmospheric parameters - i.e temperature and water vapor concentration - could have occur which would possibly explain the 1.1° C constant found in (2). Last, the observed ΔT are certainly underestimated by a factor τ, the atmospheric transmittance in the 10.5 - 12.5 µm, which is typically $\tau = 0.7$ for a midlatitude summer atmosphere.

The results may be compared to the predicted values from HASSE (1971). Using a mean solar irradiance at sea level $Q = 900\ W.m^{-2}$ in (1), ΔT is found to vary like $3.5\ U^{-1}$ (U in $m.s^{-1}$) which fits the measured values in the wind speed range 1-3.$m.s^{-1}$, but overestimates ΔT for $U < 1m.s^{-1}$. As pointed out by HASSE, the results of the model given in (1) can not be applied to the lower wind speed range because the model used by HASSE refers to a steady state assumption which is then not respected at scales of a few hours.

III-3 - Limit value of the diurnal heating

Fig. 5 and other HCMM scenes with large diurnal heatings indicate that diurnal heating do not exceed about 5° C, and that a limit value should exist at low wind speed. This value may be obtained by solving the heat transfer equation :

$$\frac{d}{dz}\left(k(z)\,\frac{dT(z,t)}{dt}\right) + \frac{dF(z,t)}{dz} = \rho c\,\frac{dT(z,t)}{dt} \qquad (3)$$

for $k(z) = k_m$ the thermal molecular diffusivity - i.e no turbulent diffusivity at $U = o$. Eq. (3) was solved using the following conditions :

$$F(z,t) = F(o,t)\ g(z) - F_o \tag{4}$$

where $F(o,t)$ is the solar irradiance at sea level, F_o the heat loss by the surface, and

$$g(z) = \sum a_i \exp(-k_i z) \tag{5}$$

where a_i, k_i are given in Table 1 and were obtained from a fit of $g(z)$ according to the work by PRUVOST (1976). $g(z)$ is taken as independent of time in (4) which is a rather good approximation since the underwater penetration of the direct solar radiation is close to the nadir even at low solar elevation angles. An homogeneous layer defined by $F(o,t)\ g(z_o) = F_o$ was set just below the surface for which $(\frac{dT}{dz}) = o$ (z_o is a few centimeters for $F_o \simeq 100\ W.m^{-2}$, $F(o,t) \simeq 1000\ W.m^{-2}$). Under these conditions, ΔT was found to vary nearly with the net heat budget of the surface :

$$\Delta T_{max} \simeq C \int_o^{t_o} (F(o,t) - F_o)\ dt \tag{6}$$

with $C = 0.65.10^{-6}\ K.j^{-1}\ m^2$. For the HCMM observations or June 3, 1978, $\int_o^{t_o} (F(o,t)-F_o).dt$ was estimated to about 600 $W.m^{-2}$ during 4 hours (in fact a maximum value of 900 $W.m^{-2}$ at noon at satellite overpass) and

$$\Delta T_{max} = 5.6\ °C \tag{7}$$

The Hasse's formula (1) may be simply accomodated to account for the limit found in (6) by writing :

$$\Delta T = 3.5\ 10^{-3}\ Q\ /\ (U_o(t) + U) \qquad (8)$$

where $U_o(t)$ wi depends of the given hour during the day. In our case, U_o should be about 0.7 $m.s^{-1}$ and when plotted in Fig. 5, Eq. (8) fits pretty well the observations.

III-4 - Frequency of diurnal heating

From May 13 to August 28, 1978, 60 HCMM scenes taken over the Westernn Mediterranean Sea were examined, of which about 34 scenes exhibited large diurnal (typically more than 1° C) heating of particular areas of 10 to 100 km width. Relative frequency of the event is rather large, and is enhanced in some areas affected by a breeze effect where the wind systematically becomes nul at some distance of the coast. Table 2 give relative frequencies of low wind speeds ($U < 3\ m.s^{-1}$) at some stations along the Coast of France during the summer months (from DARCHEN (1974)). Frequency of nul wind allowing a diurnal heating of more than 1° C are between 10 to 30 % .Frequency of low wind speed ($1 < U < 3\ m.s^{-1}$) is from 20 to 50 %, allowing a diurnal heating of about 1° C. From these frequencies, N_1 and N_2, a mean diurnal heating $\bar{\Delta T}$ was calculated as .

$$\bar{\Delta T} = 2.5\ N_1 + N_2$$

and is given also in Table 2. The mean diurnal heating ranges from 0.5 to 1.5° C along the south coast of France with a maximum on the French Riviera (Cap Ferrat).

IV - CONCLUSION

The present investigation, using SST satellite observations from the HCMM experiment has shown a high frequency of large diurnal heatings (more than 1° C) of the sea surface during summer months in such areas like the Mediterranean Sea where low wind speed are very frequent. This shows that satellite observations at noon and during the ofternoon should be rejected, or at least checked to eliminate those corresponding to low wind speed ($U < 3\ m.s^{-1}$). If not, a systematic bias could be introduced in the SST analysis of ~~same~~ some areas, particularly the marine coastal areas affected by a sea-~~l~~and breeze effect.

Using simultaneous observations of the glitter reflectance, the diurnal heating was correlated to the wind speed. Diurnal heatings of about 1° C were found for $U \simeq 2\ m.s^{-1}$, which fits the formulation given by HASSE (1971). A maximum diurnal heating of 5° C is found for nul wind conditions, which is in agreement to the value calculated from the radiative and heat transfer, assuming the thermal diffusivity is only molecular.

APPENDIX

Glitter refers to direct solar radiation reflected by the sea surface. This reflection is specular for a planar surface. When there is wind, the surface is agitated and consists of elements which are statistically distributed around the horizontal plane. This produces a more or less bright spot of variable dimensions which is commonly called glitter.

The radiance L_g reflected by the agitated sea surface can be expressed (COX and MUNK, 1956)

$$L_g = \frac{E_s}{4} \frac{R(\omega)}{\mu_v \mu_n^4} p \qquad \text{(A-1)}$$

and the equivalent reflectance ρ_g will be expressed as

$$\rho_g = \frac{\pi L_g}{\mu_s E_s} = \frac{\pi}{4} \frac{R(\omega)}{\mu_s \mu_v \mu_n^4} p \qquad \text{(A-2)}$$

where E_s is the direct solar radiation at sea level,

$R(\omega)$ is the reflection coefficient of water at a given indicence ω,

p is the probability of encountering a properly oriented surface element,

$\mu_v = \cos\Theta_v$, $\mu_s = \cos\Theta_s$, $\mu_n = \cos\Theta_n$, respectively define the zenithal angles of the observation direction, the direction of incidence, and their bisector,

φ is the angle between the planes of incidence and observation :

$$\mu_n = \frac{\mu_s+\mu_v}{2\cos\omega} \qquad \text{(A-3)}$$

$$\cos 2\omega = \mu_s\mu_v+\left(1-\mu_s^{\;2}\right)^{\frac{1}{2}}\left(1-\mu_v^{\;2}\right)^{\frac{1}{2}}\cos\varphi \qquad \text{(A-4)}$$

From a study of aerial photographs of glitter patterns, COX and MUNK (1955) developped p in a Gram Charlier series which in a first approximation is reduced to a gaussian distribution , with revolution symmetry :

$$p = \frac{1}{\Pi\sigma^2} \exp - \frac{(tg\ \Theta_n)^2}{\sigma^2} \qquad \text{(A-5)}$$

$$\text{with } \sigma^2 = 0{,}003 + 5{,}12.10^{-3}U_{m.s}{}^{-1} \pm 0{,}004 \qquad \text{(A-6)}$$

for $1 < U < 14\ m.s^{-1}$

Figure 6 gives an example of the glitter spot ρ_g thus computed as a function of solar zenithal angle for different values of W, and for a nadir viewing ($\Theta_v = 0$). In accordance with the reciprocity principle, by permutation ($\Theta_s ; \Theta_v$), Fig.6 also gives ρ_g as a function of observation angle for a sun at the zenith ($\Theta_s = 0$). For a given angle ρ_g presents a maximum, ρ_{gm}, at a certain value of σ_m which is related to wind speed. σ_m and ρ_{gm} are given by :

$$\sigma_m^{\;2} = tg^2\Theta_n = \mu_n^{\;-2}-1 \qquad \text{(A-7)}$$

$$\rho_{gm} = \frac{R(\omega)}{4\ \mu_s\mu_v\mu_n^{\;2}\ (1-\mu_n^{\;2})} \qquad \text{(A-8)}$$

The dashed curve in Fig.6 envelops the preceeding curves and represents the maximum glitter ρ_{gm} as defined by (A-8).

REFERENCES

1 - COX, C., MUNK, W., 1955 - Slopes of the sea surface deduced from photographes of the sum glitter. Bulletin of the Scripps Institution of Oceanography, California, 6 (9), 401-488.

2 - COX, C., MUNK, W., 1956 - Journal of Marine Research 14 (1), 63-78.

3 - DARCHEN, J., 1974 - Éléments climatologiques concernant les côtes de la France métropolitaine (Méditerranée). Monographie n° 93 de la Météorologie Nationale, France.

4 - HASSE, L., 1971 - The sea surface temperature deviation and the heat flow at the sea-air interface. Boundary Layer Meteorology 1, 368-379.

5 - LA VIOLETTE, P.E., PETEHERYCH, S., GOWER, J.F.R., 1980 - Oceanographic implications of features in NOAA satellite visible imagery. Boundary Layer Meteorology 18, 159-175.

6 - PRUVOST, P., 1975 - Etude du flux solaire et de l'échauffement radiatif dans la mer par temps clair. Annales Hydrologiques 5ème série vol. 3 (1), 25-34.

7 - ROMER, J., 1969 - Variations de la température de surface de la mer au voisinage de la surface. Note EERM n° 262, Météorologie Nationale, France.

8 - STOMMEL, H., SAUNDERS, K., SIMMONS, W., COOPER, J., 1969 - Observations of the diurnal thermocline. Deep Sea Research, Supplement vol. 16, 269-284.

Table 1 - Coefficients a_i, k_i in (5) for solar irradiance underwater penetration.

	a_i	$k_i\,(m^{-1})$
i = 1	.041	3365.9
i = 2	.139	201.18
i = 3	.211	13.05
i = 4	.24	1.22
i = 5	.37	.07

Table 2 - Relative frequencies of low wind speeds :

N_1 : nul ; N_2 : Beaufort forces 1 and 2 ($1 < U < 3$ m.s^{-1}), during June, July and August in the french mediterranean coastal area from DARCHEN (1974). An estimate of the mean diurnal heating $\overline{\Delta T}$ is given in column (3).

Station	N_1 %	N_2 %	$\overline{\Delta T}$ °C
Cap Bear	16.0	26.9	0.67
Sète	9.5	42.3	0.66
Panègues	21.3	26.8	0.80
Cap Camarat	10.8	46.6	0.74
Cap Ferrat	35.1	50.4	1.38
Cap Corse	18.4	35.5	0.82
Pertusato	6.4	21.0	0.37
42° N-6E	7.6	/	0.5 ?

FIGURES CAPTIONS

Figure 1 - Diurnal heating in the Western Mediterranean Sea :

(a) - HCMM scene A-A0038 - 12440 on June 3, 1978 at 12.40 TU, image center is at 40.54 N, 011.04 E. Visible channel : darker tones are is lower reflectances. Note the bright patterns East and West of Corsica and Sardina.

(b) - Same as (a) but infrared channel : darker tones are colder sea surface temperatures. Note warmer waters East of Corsica and Sardina.

(c) - Day-night temperature differences between HCMM scenes obtained on June 3, 1978 at 1.50 TU (night) and 12.40 TU (day). Darker tones are smaller diurnal heatings.

(d) - Meteorological situation, on June 3, 1978 at 12.00 TU.

Figure 2 - Diurnal heating in the North Sea :

(a) - Day HCMM scene A-A0034 - 13120, on May 30, 1978 at 13.10 TU. Image center is at 54.27 N, 00.01E. Infrared channel : darker tones are colder waters. Note the warm (bright) spot between Scotland and the top right of the image where a thermal front is shown close to Norway.

(b) - Night HCMM scene A-A0035 - 02280, on May 31, 1978 at 2.30 TU. Image center is at 56.13 - 03.00E. Infrared channel : darker tones are colder waters. The warm spot disappeared during the night.

(c) - Meteorological situation on May 30, 1978.

Figure 3 - Day-night temperature difference vs glitter reflectance on June 3, 1978, for a study area East of Sardina.

Figure 4 - Retrieved wind speed vs glitter reflectance for the study area.

Figure 5 - Day-night temperature difference vs retrieved wind speed for the study area. Dasked line is from HASSE (1971). Full line is (8) : the HASSE's formula after modification to account for a low wind speed limit of ΔT.

Figure 6 - Glitter reflectance vs zenithal viewing angle, for a sun at zenith, and several wind speeds from 0 to 15 $m.s^{-1}$. Maximum glitter reflectance is given by a dashed line.

FIG. 1a

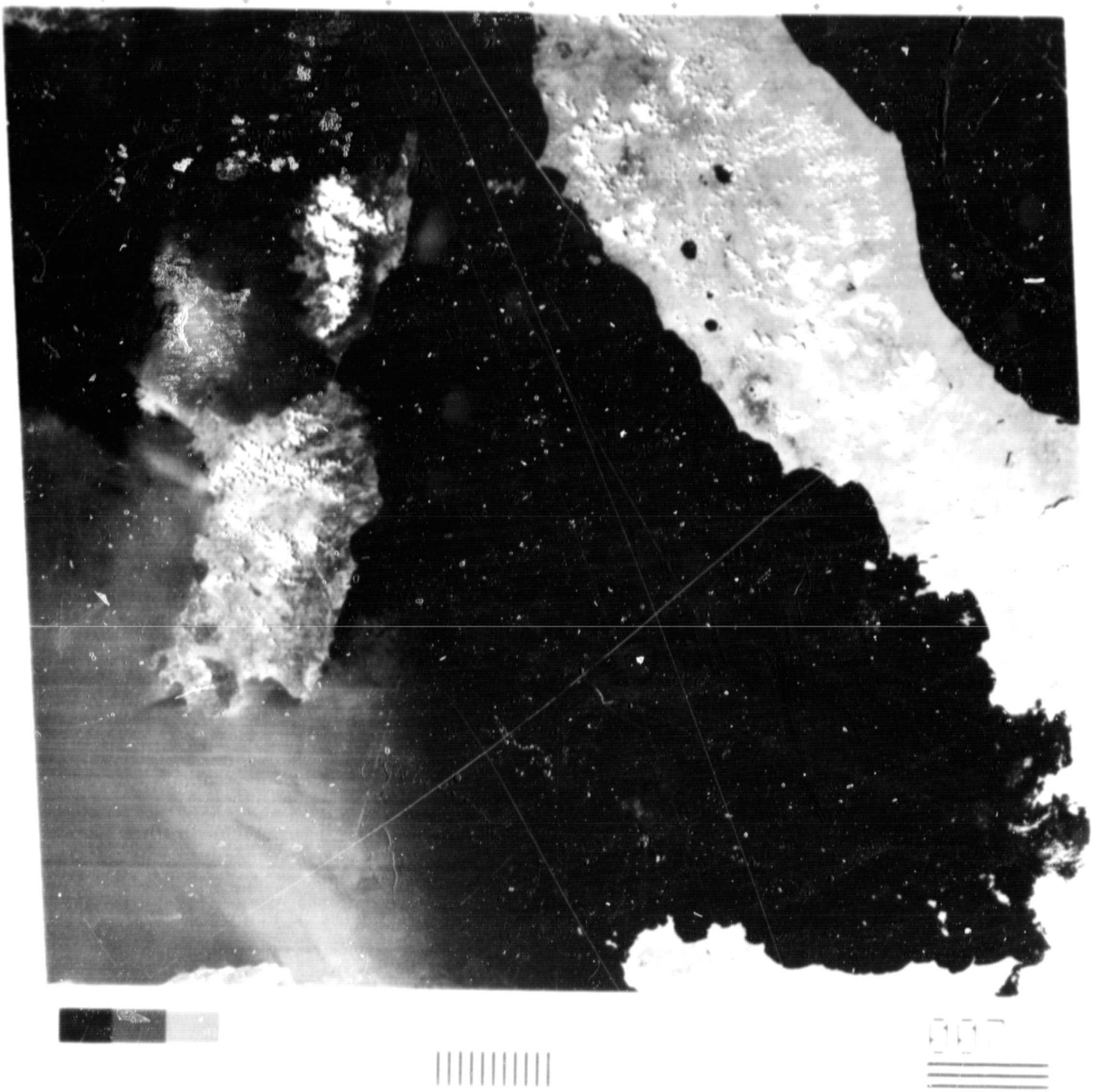

FIG 1b

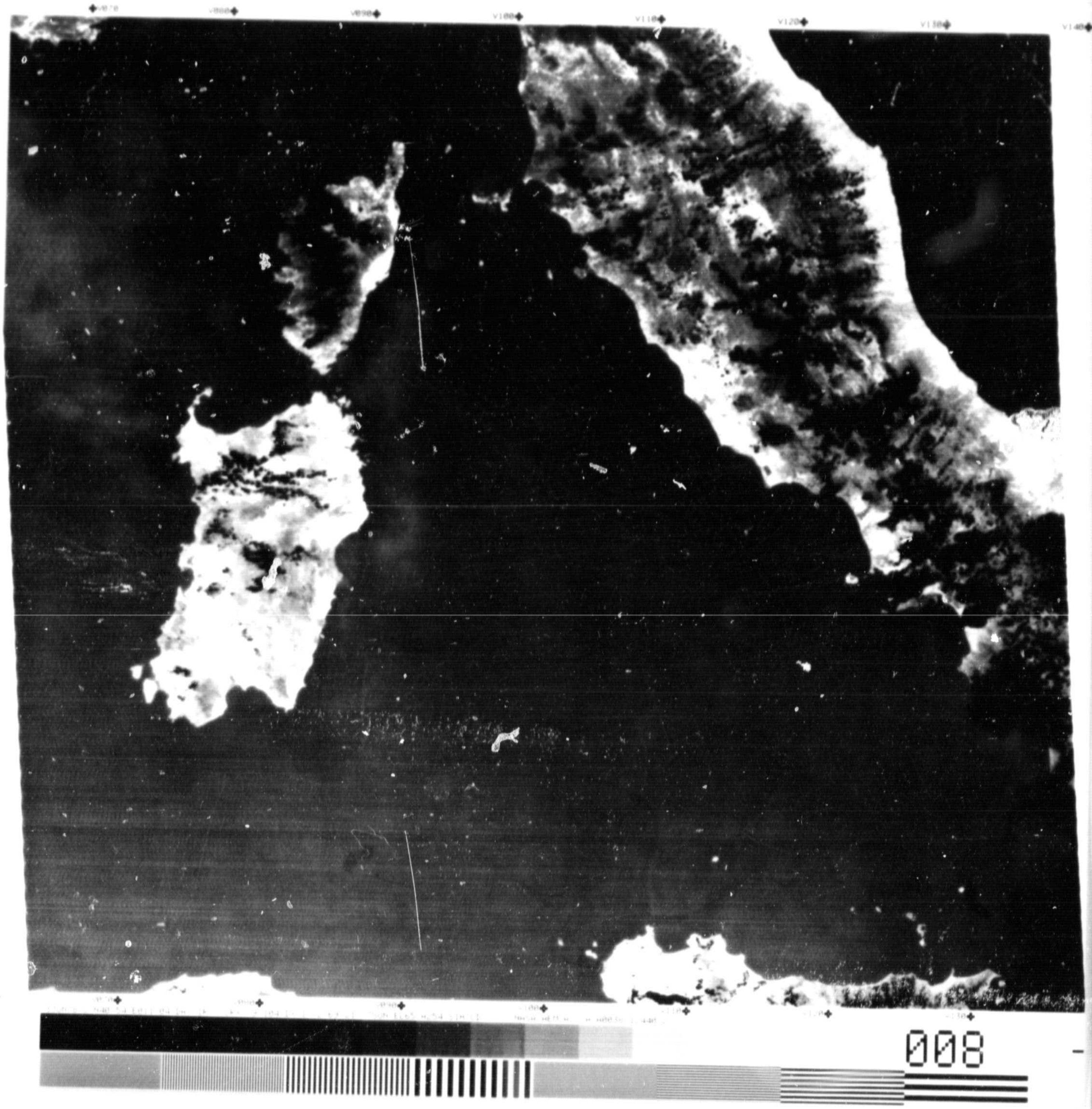

FIG. 1c

FIG. 1d

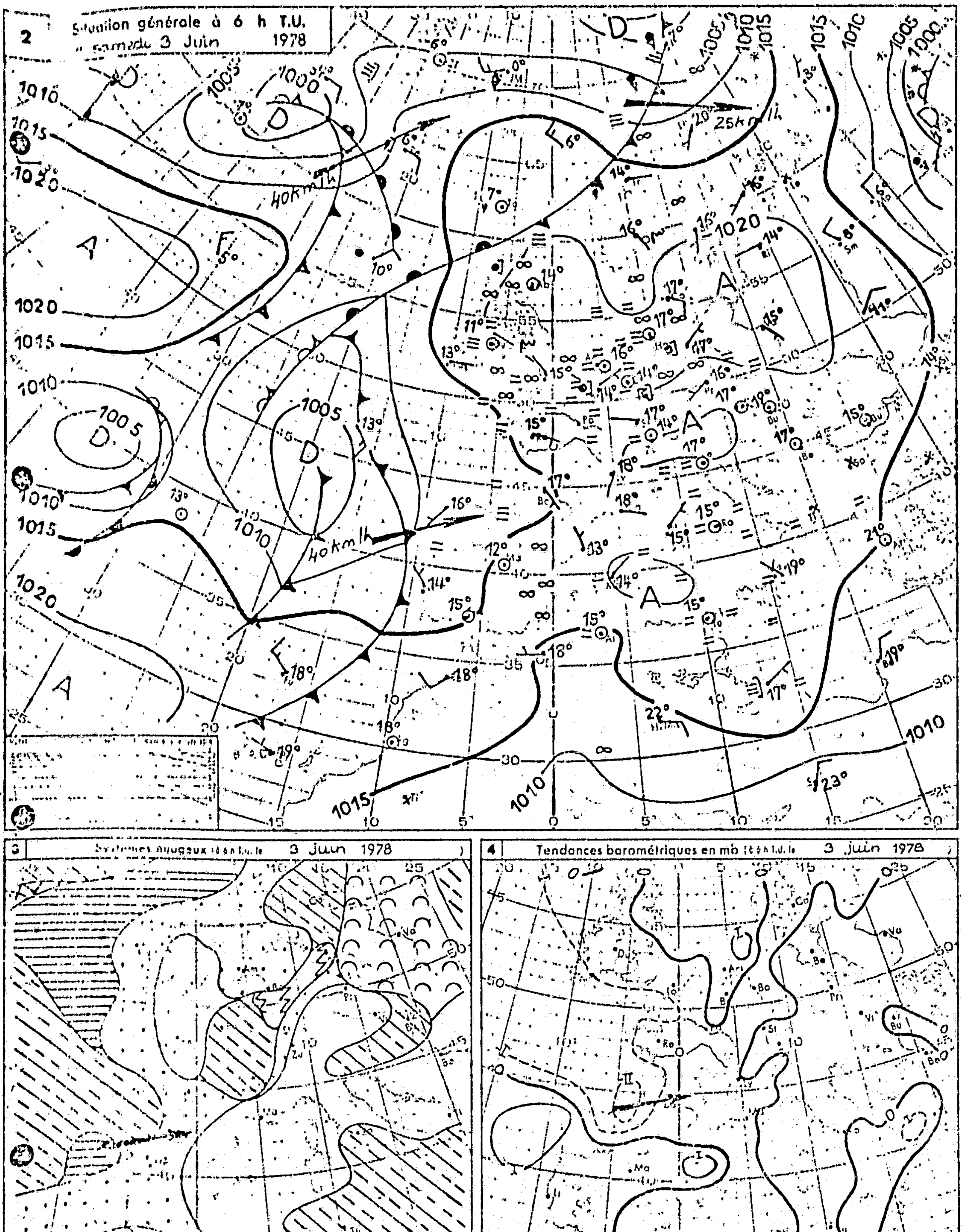
2
Situation générale à 6 h T.U.
samedi 3 Juin 1978
40km/h
25km/h
3
3 Juin 1978
4
Tendances barométriques en mb
3 juin 1978

FIG. 2a

ORIGINAL PAGE IS
OF POOR QUALITY

FIG. 2b

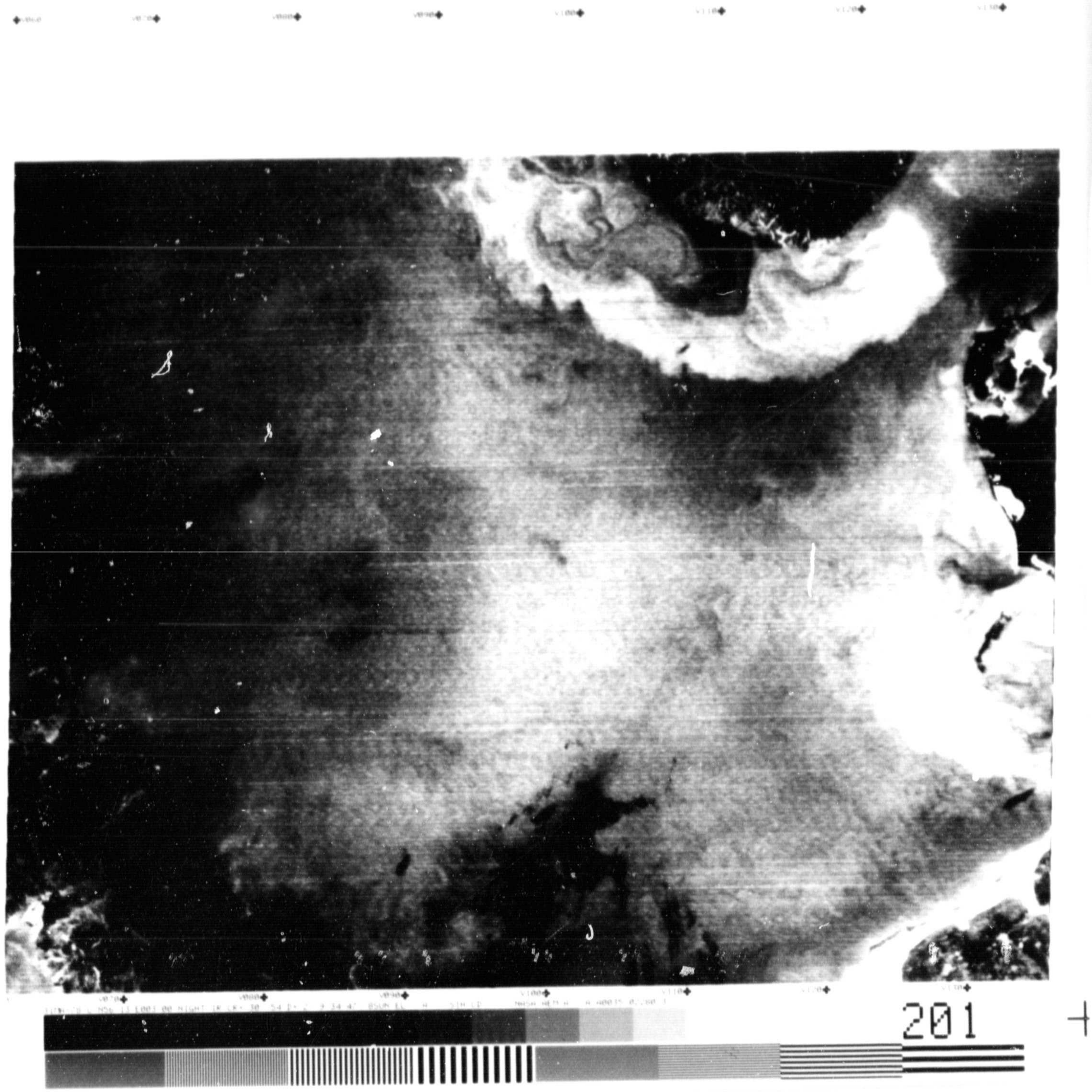

FIG. 2c

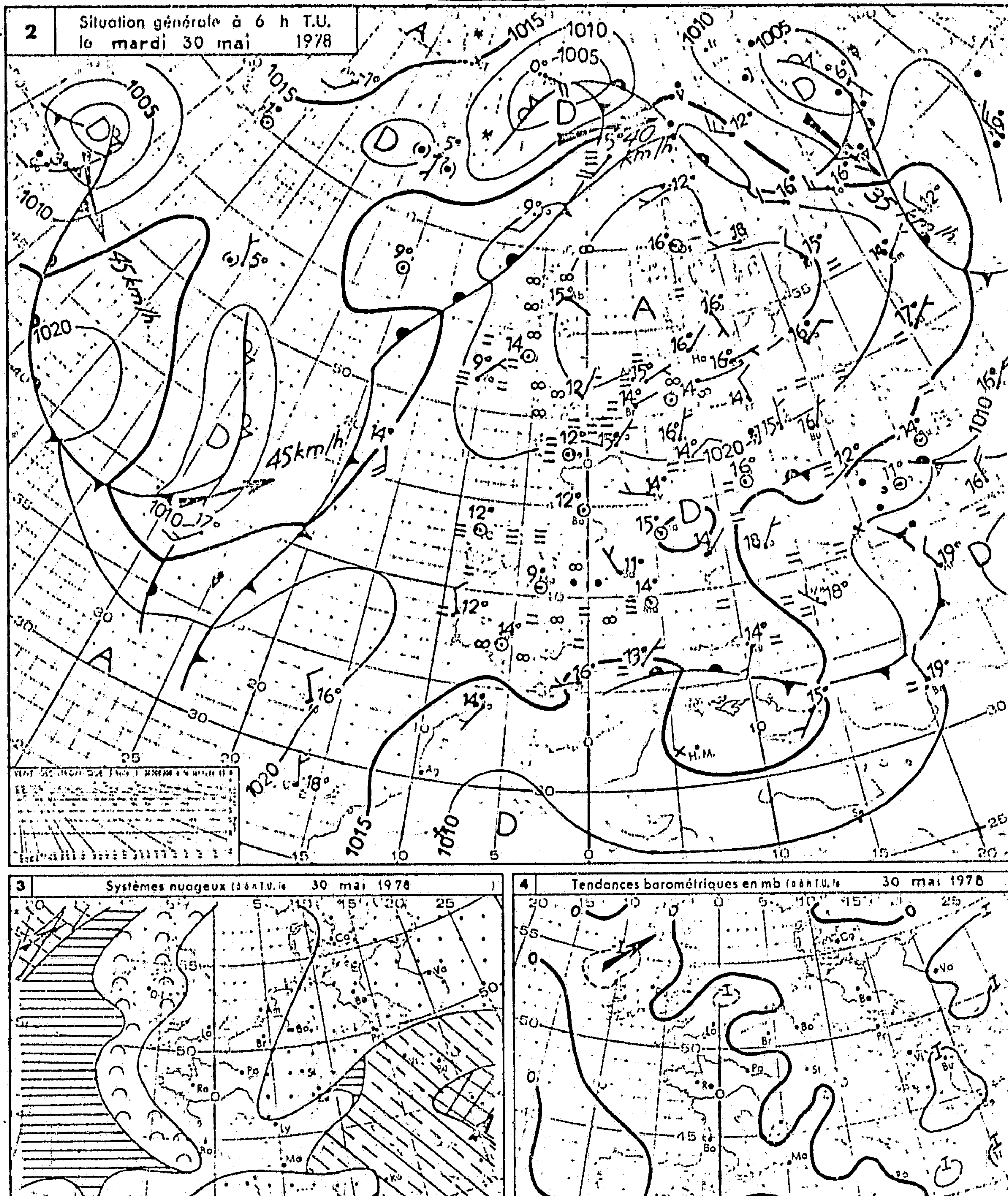
2
Situation générale à 6 h T.U.
le mardi 30 mai 1978
45km/h
3
Systèmes nuageux (à 6 h T.U.) 30 mai 1978
4
Tendances barométriques en mb (à 6 h T.U.) 30 mai 1978

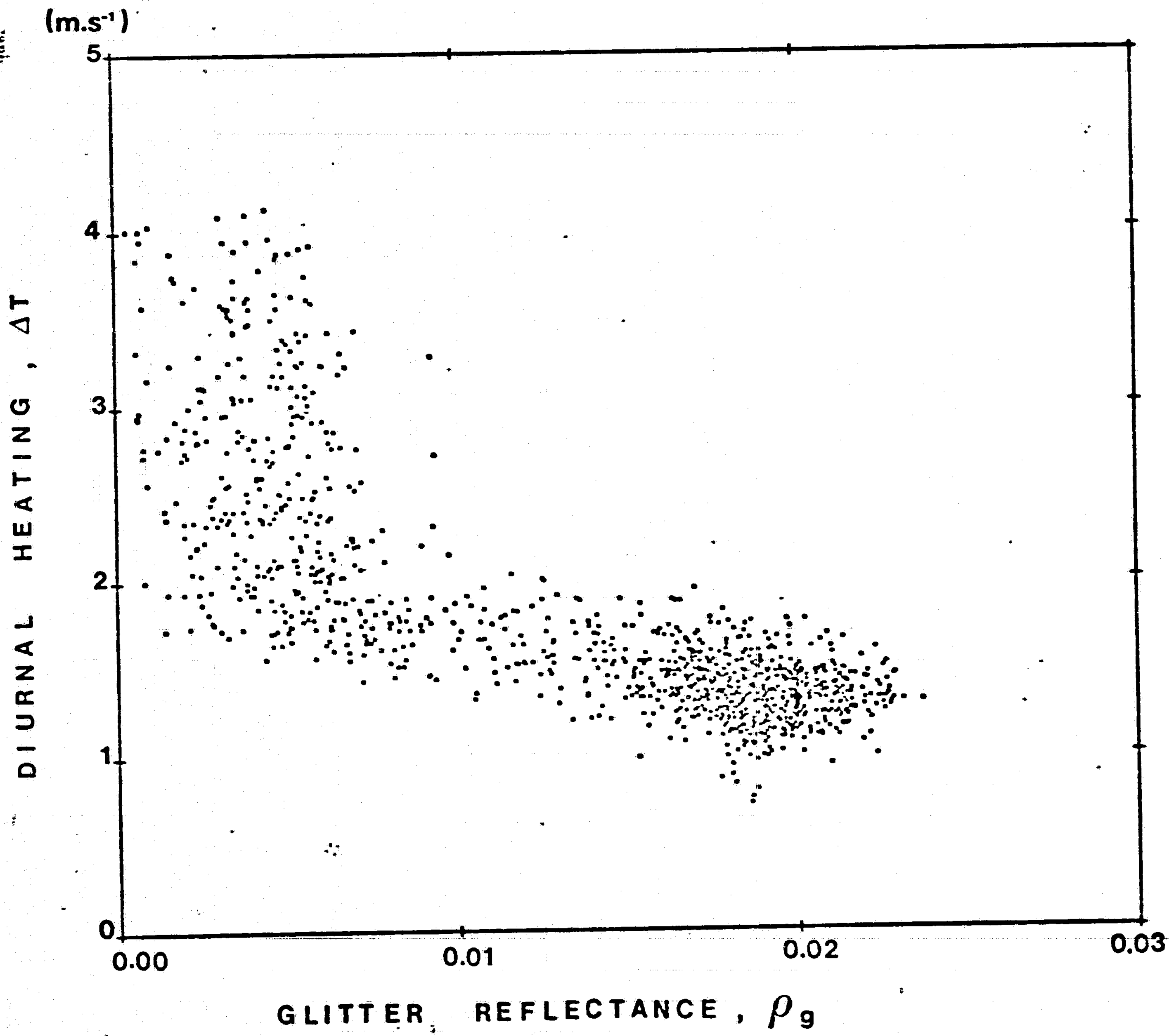
(m.s⁻¹)
DIURNAL HEATING , ΔT
0
1
2
3
4
5
0.00
0.01
0.02
0.03
GLITTER REFLECTANCE , ρ_g

FIG. 3

FIG. 4

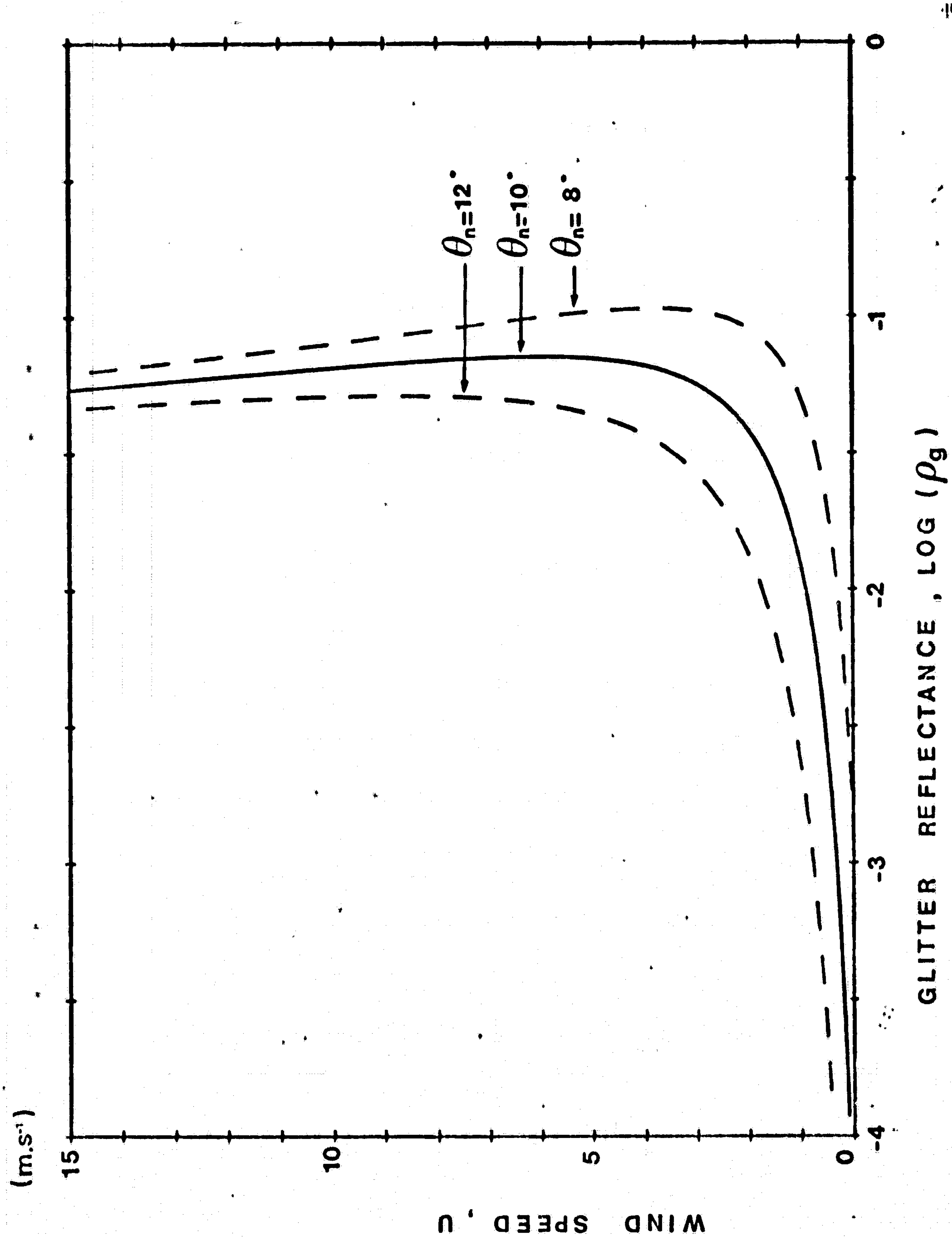

WIND SPEED, U (m.s⁻¹)
GLITTER REFLECTANCE, LOG (ρ_g)
θ_n=12°
θ_n=10°
θ_n= 8°
15
10
5
0
-4
-3
-2
-1
0

FIG. 5

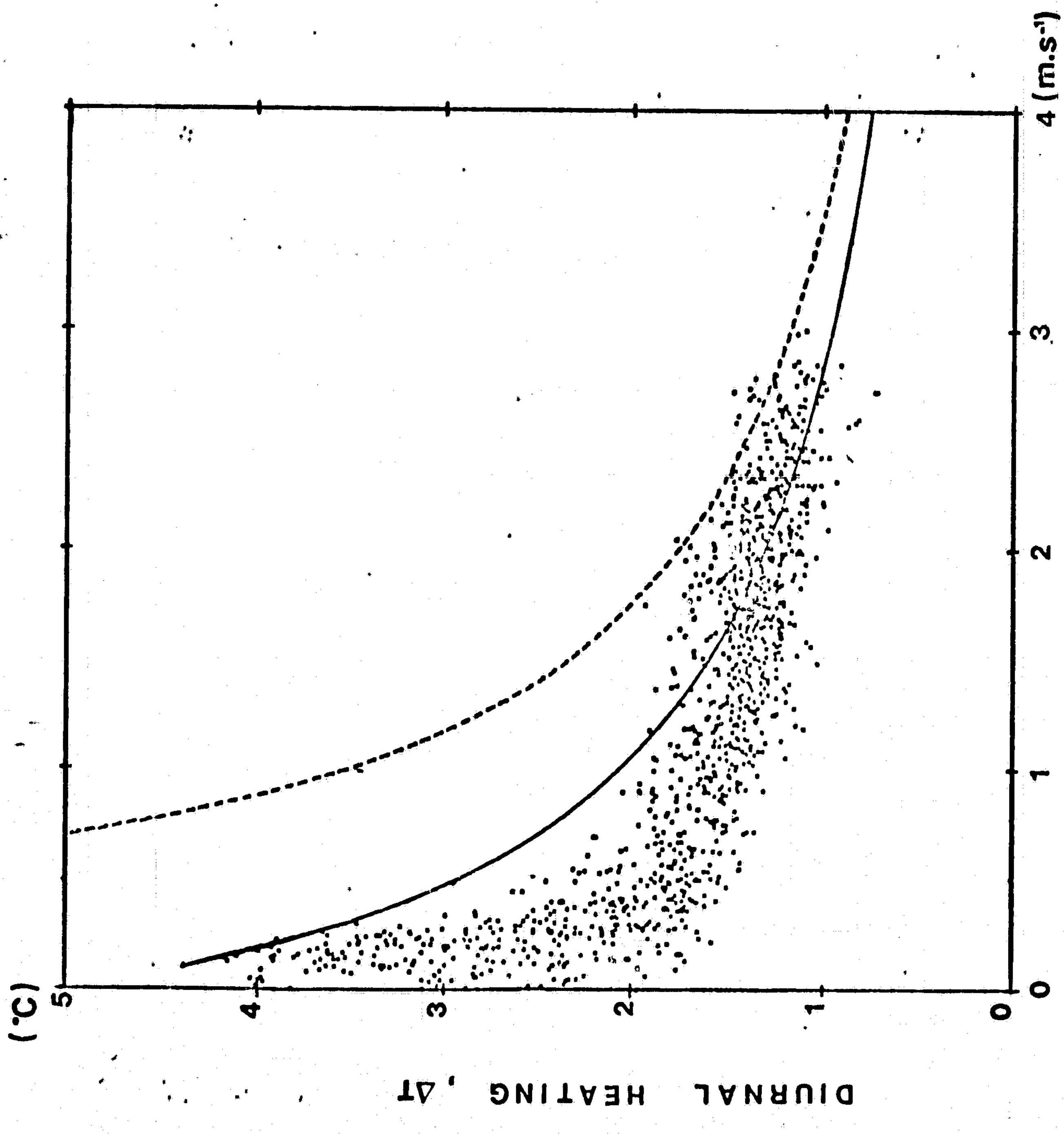

Fig. 6

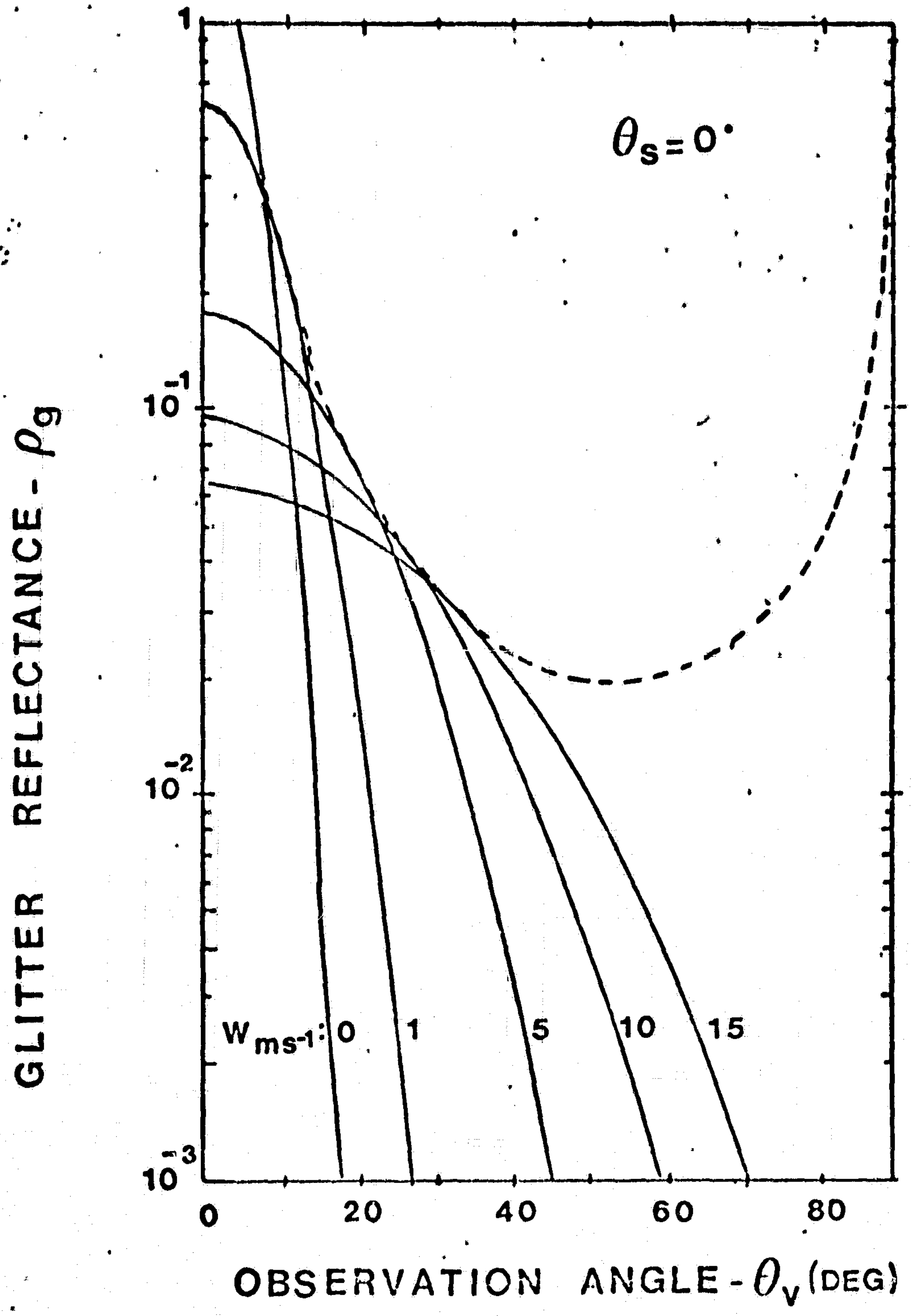

$\theta_s = 0°$
GLITTER REFLECTANCE - ρ_g
OBSERVATION ANGLE - θ_v (DEG)
1
10^{-1}
10^{-2}
10^{-3}
0
20
40
60
80
$W_{ms^{-1}}$: 0 1 5 10 15

'ani·
'ani·

The following listing give the date, identification and location of center of image of HCMM scenes received from NASA by the Principal Investigator. The last column "ETAT" give the status of the corresponding digital data :

- R : received
- IR : received but not readable
- C : requested but not received.

DATE	IDENTIFICATION	LOCATION		SCENE	BDE	ETAT	UST	PM
11MAY78	15- 2540-3	53.32N	3.43W					
11MAY78	15- 2550-3	47.29N	6.08W		303	R	M	2
11MAY78	15- 2560-3	45.29N	6.08W		303	R	M	8
11MAY78	15- 2564-3	41.10N	8.45W					
11MAY78	15- 2570-3	41.26N	8.08W		303	R	M	5
11MAY78	15- 3000-3	32.50N	10.00W					
11MAY78	15-13510-1	40.35N	4.53W		318	R	M	8
11MAY78	15-13510-2	40.35N	4.53W		318	R	M	11
11MAY78	15-13530-1	46.38N	6.52W		318	R	M	2
11MAY78	15-13530-2	46.38N	6.52W		318	R	M	5
11MAY78	15-13550-1	52.40N	9.14W					
11MAY78	15-13550-2	52.40N	9.14W					
13MAY78	17- 1570-3	38.02N	5.56E		318	R	M	14
13MAY78	17-12510-1	41.29N	9.56E		318	R	M	17
13MAY78	17-12510-2	41.29N	9.56E		318	R	M	20
13MAY78	17-12540-1	53.34N	5.29E					
13MAY78	17-12540-2	53.34N	5.29E					
14MAY78	18- 2140-3	44.02N	3.10E			C		
14MAY78	18- 2150-3	37.56N	1.19E			C		
14MAY78	18-13080-1	39.07N	6.02E		312	R	M	8
14MAY78	18-13080-2	39.07N	6.02E		312	R	M	11
14MAY78	18-13100-1	45.11N	4.08E		312	R	M	2
14MAY78	18-13100-2	45.11N	4.08E		312	R	M	5
16MAY78	20- 2480-3	51.39N	3.11W		318	R	M	23
16MAY78	20- 2500-3	45.36N	5.28W		318	R	M	26
18MAY78	22- 325[illegible]-3	50.16N	12.55W					
18MAY78	22-124[illegible]-1	44.55N	10.11E					
18MAY78	22-12460-2	44.55N	10.11E					
18MAY78	22-12470-1	50.58N	7.57E		312	R	M	14
18MAY78	22-12470-2	50.58N	7.57E		312	R	M	17
19MAY78	23- 2050-3	55.24N	9.04E					
19MAY78	23- 2080-3	43.19N	4.20E					
19MAY78	23- 2100-3	37.13N	2.31E					
19MAY78	23-13050-2	50.25N	3.35E					
20MAY78	24-13200-1	38.07N	3.07E					
20MAY78	24-13200-1	36.32N	3.34E					
20MAY78	24-13200-2	38.07N	3.07E					
20MAY78	24-13200-2	36.32N	3.34E					
20MAY78	24-13220-1	44.11N	1.15E					
20MAY78	24-13220-2	44.11N	1.15E					
20MAY78	24-13230-1	48.40N	.19E		293	R	M	8
20MAY78	24-13230-1	50.13N	.56E		293	R	M	2
20MAY78	24-13230-2	48.40N	.19E		293	R	M	11
20MAY78	24-13230-2	50.13N	.56E		293	R	M	5
20MAY78	24-13250-1	54.40N	2.52W		293	R	M	20
20MAY78	24-13250-1	56.14N	3.37W		293	R	M	14
20MAY78	24-13250-2	54.40N	2.52W		293	R	M	23
20MAY78	24-13250-2	56.14N	3.37W		293	R	M	17
21MAY78	25-13380-1	35.53N	.52E					
21MAY78	25-13380-2	35.53N	.52E					

ORIGINAL PAGE IS
OF POOR QUALITY

DATE	IDENTIFICATION	LOCATION		SCENE	DDE	ETAT	DST	PM
21MAY78	25-13390-1	41.58N	2.38W					
21MAY78	25-13390-2	41.58N	2.38W					
21MAY78	25-13410-1	48.01N	4.41W		312	R	M	20
21MAY78	25-13410-2	48.01N	4.41W		312	R	M	23
21MAY78	25-13430-1	54.04N	7.08E					
21MAY78	25-13430-2	54.04N	7.08E					
22MAY78	26- 3000-3	52.30N	6.02W			C		
22MAY78	26- 3020-3	46.27N	8.23W			C		
23MAY78	27- 1440-3	42.47N	10.07E					
23MAY78	27- 1440-3	42.28N	10.01E					
23MAY78	27- 1450-3	36.40N	8.19E					
23MAY78	27- 1450-3	36.22N	8.14E					
23MAY78	27- 3180-3	52.55N	10.27W					
23MAY78	27- 3200-3	46.52N	12.50W		318	R	M	29
24MAY78	28- 2020-3	43.47N	5.49E		320	R	M	2
24MAY78	28- 2030-3	37.41N	3.58E					
24MAY78	28-12550-1	36.16N	9.35E					
24MAY78	28-12550-2	36.16N	9.35E					
24MAY78	28-12570-1	42.40N	7.47E		312	R	M	26
24MAY78	28-12570-2	42.40N	7.47E		312	R	M	29
25MAY78	29- 2210-3	39.37N	.02E		320	R	M	5
25MAY78	29-13140-1	37.22N	4.40E					
25MAY78	29-13140-1	37.40N	4.35E					
25MAY78	29-13140-2	37.22N	4.40E					
25MAY78	29-13140-2	37.40N	4.35E					
25MAY78	29-13150-1	43.26N	2.50E			C		
25MAY78	29-13150-2	43.26N	2.50E			C		
25MAY78	29-13170-1	49.29N	.42E					
25MAY78	29-13170-1	49.47N	.35E		310	R	M	26
25MAY78	29-13170-2	49.29N	.42E					
25MAY78	29-13170-2	49.47N	.35E		310	R	M	29
26MAY78	30- 2370-3	48.31N	1.41W		320	R	M	8
26MAY78	30- 2380-3	42.26N	3.45W		320	R	M	11
26MAY78	30-13310-1	35.27N	.39E					
26MAY78	30-13310-2	35.27N	.39E					
26MAY78	30-13330-1	41.32N	1.06W					
26MAY78	30-13330-2	41.32N	1.06W					
26MAY78	30-13350-1	47.36N	3.08W			C		
26MAY78	30-13350-2	47.36N	3.08W			C		
26MAY78	30-13360-1	53.38N	5.34W					
26MAY78	30-13360-2	53.38N	5.34W					
27MAY78	31- 2540-3	50.25N	5.32W		320	R	M	14
27MAY78	31- 2560-3	44.21N	7.44W		320	R	M	17
27MAY78	31-13510-1	40.50N	5.28W					
27MAY78	31-13510-2	40.50N	5.28W					
27MAY78	31-13530-1	46.54N	7.27W			C		
27MAY78	31-13530-2	46.54N	7.27W			C		
27MAY78	31-13540-1	52.56N	9.50W					
27MAY78	31-13540-2	52.56N	9.50W					
25MAY78	32- 3120-3	57.05N	9.00W					

63

DATE	IDENTIFICATION	LOCATION		SCENE	BDE	ETAT	DST	PM	
28MAY78	32- 3180-3	47.02N	11.23W						
28MAY78	32-12350-1	50.08N	11.02E						
28MAY78	32-12350-1	51.38N	10.26E						
28MAY78	32-12350-2	50.08N	11.02E						
28MAY78	32-12350-2	51.38N	10.26E						
28MAY78	32-12360-1	56.08N	8.22E		320	R	M	20	
28MAY78	32-12360-2	56.08N	8.22E		320	R	M	23	
28MAY78	32-14110-1	46.49N	12.01W						
28MAY78	32-14110-2	46.49N	12.01W						
29MAY78	33- 1550-3	43.35N	7.08E		303	R	M	11	
29MAY78	33- 1570-3	57.29N	5.18E						
29MAY78	33-12500-1	59.56N	9.57E		293	R	M	26	
29MAY78	33-12500-2	59.56N	9.57E		293	R	M	29	
29MAY78	33-12520-1	46.01N	7.59E		294	R	M	2	
29MAY78	33-12520-2	46.01N	7.59E		294	R	M	5	
29MAY78	33-12530-1	52.03N	5.40E		320	R	M	26	
29MAY78	33-12530-2	52.03N	5.40E		320	R	M	29	
30MAY78	34- 2120-3	50.41N	5.06E		303	R	M	14	
30MAY78	34- 2120-4	43.32N	4.14E		328	R	M	7	****
30MAY78	34- 2120-5	43.32N	4.14E		328	R	M	10	****
30MAY78	34- 2120-6	43.32N	4.14E		333	R	M	2	****
30MAY78	34- 2120-7	43.32N	4.14E		333	R	M	5	****
30MAY78	34- 2120-8	36.56N	.36E		328	R	M	4	****
30MAY78	34- 2130-3	44.37N	2.53E		303	R	M	17	
30MAY78	34- 2130-3	50.05N	4.30E						
30MAY78	34- 2140-3	44.37N	2.53E			C			
30MAY78	34- 2150-3	38.31N	1.02E						
30MAY78	34- 2280-3	56.13N	3.00E			C			
30MAY78	34-13070-1	56.17N	6.25E						
30MAY78	34-13070-2	56.17N	6.25E						
30MAY78	34-13080-1	58.50N	5.41E		294	R	M	8	
30MAY78	34-13080-2	58.50N	5.41E		294	R	M	11	
30MAY78	34-13090-1	44.55N	3.47E		304	R	M	5	
30MAY78	34-13090-1	42.22N	4.37E		304	R	M	2	
30MAY78	34-13090-2	44.55N	3.47E		304	R	M	8	
30MAY78	34-13090-2	42.22N	4.37E						
30MAY78	34-13100-1	48.26N	2.32E		303	R	M	26	
30MAY78	34-13100-2	48.26N	2.32E		303	R	M	29	
30MAY78	34-13110-1	50.58N	1.33E		321	R	M	2	
30MAY78	34-13110-2	50.58N	1.33E		321	R	M	5	
30MAY78	34-13120-1	54.27N	.01E		303	R	M	20	
30MAY78	34-13120-2	54.27N	.01E		303	R	M	23	
31MAY78	35- 2280-3	56.13N	3.00E		313	R	M	14	
31MAY78	35- 2300-3	50.47N	.34E		313	R	M	17	
31MAY78	35- 2300-3	50.11N	.19E			C			
31MAY78	35- 2310-3	44.43N	1.38W			C			
31MAY78	35- 2320-3	44.07N	1.50W			C			
31MAY78	35- 2330-3	38.01N	3.41W						
31MAY78	35- 2330-3	38.37N	7.30W						
31MAY78	35-21320-1	35.40N	110.30W		304	R	M	11	

DATE	IDENTIFICATION	LOCATION		SCENE	RDE	ETAT	DST	PM	
31MAY78	35-21320-2	55.40N	119.30W		304	R	M	14	
1JUN78	36- 2480-3	51.25N	3.44W						
1JUN78	36- 2490-3	45.21N	6.00W						
1JUN78	36-13440-1	38.45N	3.23W		321	R	M	14	
1JUN78	36-13440-2	38.35N	3.23W		321	R	M	17	
1JUN78	36-13460-1	42.00N	4.25W						
1JUN78	36-13460-1	44.40N	5.17W		321	R	M	8	
1JUN78	36-13460-2	42.00N	4.25W						
1JUN78	36-13460-2	44.40N	5.17W		321	R	M	11	
1JUN78	36-13470-1	50.43N	7.31W						
1JUN78	36-13470-2	50.43N	7.31W						
2JUN78	37- 3060-3	51.12N	8.25W						
2JUN78	37- 3080-3	45.08N	10.41W						
3JUN78	38- 1480-4	43.39N	10.11E		331	R	M	7	****
3JUN78	38- 1480-5	43.39N	10.11E		334	R	M	4	****
3JUN78	38- 1480-6	43.39N	10.11E		330	R	M	5	****
3JUN78	38- 1480-7	43.39N	10.11E		330	R	M	8	****
3JUN78	38- 1480-8	54.52N	5.59E		331	R	M	4	****
3JUN78	38- 1490-3	41.46N	7.56E		294	R	M	14	
3JUN78	38- 1510-3	55.39N	6.11E						
3JUN78	38-12440-1	40.54N	11.04E		304	R	M	29	
3JUN78	38-12440-2	40.54N	11.04E			C			
3JUN78	38-12460-1	46.59N	9.04E		304	R	M	23	
3JUN78	38-12460-2	46.59N	9.04E		304	R	M	26	
3JUN78	38-12470-1	53.01N	6.40E		304	R	M	17	
3JUN78	38-12470-2	53.01N	6.40E		304	R	M	20	
4JUN78	39- 2040-3	55.46N	8.44E						
4JUN78	39- 2050-3	49.44N	6.06E						
4JUN78	39- 2070-3	43.39N	3.57E						
4JUN78	39- 2090-3	57.32N	2.07E			C			
4JUN78	39-13020-1	59.56N	6.47E			C			
4JUN78	39-13020-2	59.56N	6.47E			C			
4JUN78	39-13030-1	46.01N	4.49E						
4JUN78	39-13030-2	46.01N	4.49E						
4JUN78	39-13050-1	52.03N	2.29E			C			
4JUN78	39-13050-2	52.03N	2.29E			C			
5JUN78	40- 2220-3	55.30N	4.03E			C			
5JUN78	40- 2250-3	43.23N	.41E						
5JUN78	40- 2270-3	37.16N	2.30W						
5JUN78	40-13200-1	40.52N	1.56E						
5JUN78	40-13200-2	40.52N	1.56E						
5JUN78	40-13220-1	46.56N	.02E						
5JUN78	40-13220-2	46.56N	.02E						
5JUN78	40-13240-1	52.59N	2.26W						
5JUN78	40-13240-2	52.59N	2.26W						
6JUN78	41-13770-1	55.23N	1.05W			C			
6JUN78	41-13370-2	55.23N	1.05W			C			
6JUN78	41-13390-1	41.29N	2.51W						
6JUN78	41-13390-2	41.29N	2.51W						
6JUN78	41-13400-1	47.33N	4.53W			C			

ORIGINAL PAGE IS
OF POOR QUALITY

DATE	IDENTIFICATION	LOCATION		SCENE	BDE	ETAT	DST	PM
6JUN78	41-13400-2	47.33N	4.53W			C		
7JUN78	42- 3020-3	42.24N	10.08W					
8JUN78	43- 3190-3	46.00N	13.32W					
8JUN78	43-12370-1	34.45N	14.15E					
8JUN78	43-12380-1	41.20N	12.20E		294	R	M	17
8JUN78	43-12380-2	41.20N	12.20E		294	R	M	20
9JUN78	44- 1590-3	50.04N	7.40E					
9JUN78	44- 2010-3	43.59N	5.30E					
9JUN78	44- 2020-3	37.53N	3.40E					
9JUN78	44-12250-1	38.41N	8.34E					
9JUN78	44-12550-2	38.41N	8.34E					
9JUN78	44-12570-1	44.46N	6.40E					
9JUN78	44-12570-2	44.46N	6.40E					
9JUN78	44-12580-1	50.50N	4.26E					
9JUN78	44-12580-2	50.50N	4.26E					
10JUN78	45-13130-1	36.36N	4.35E					
10JUN78	45-13130-2	36.36N	4.35E					
10JUN78	45-13140-1	42.41N	2.46E					
10JUN78	45-13140-2	42.41N	2.46E					
10JUN78	45-13160-1	48.46N	.40E		307	R	M	2
10JUN78	45-13160-2	48.46N	.40E		307	R	M	5
10JUN78	45-13180-1	54.47N	1.52W					
10JUN78	45-13180-2	54.47N	1.52W					
11JUN78	46-13310-1	35.45N	.16E		313	R	M	26
11JUN78	46-13310-2	35.45N	.16E		313	R	M	29
11JUN78	46-13320-1	41.50N	1.29E			C		
11JUN78	46-13320-2	41.50N	1.29W			C		
11JUN78	46-13340-1	47.55N	3.33W		313	R	M	20
11JUN78	46-13340-2	47.55N	3.33W		313	R	M	23
11JUN78	46-13360-1	53.57N	6.02W			C		
11JUN78	46-13360-2	53.57N	6.02W			C		
12JUN78	47-13500-1	42.12N	6.13W			C		
12JUN78	47-13500-2	42.12N	6.13W			C		
12JUN78	47-13520-1	48.16N	8.17W			C		
12JUN78	47-13520-2	48.16N	8.17W			C		
13JUN78	48- 1370-3	41.26N	10.41E			C		
13JUN78	48- 3110-3	52.49N	9.28W					
13JUN78	48- 3120-3	46.46N	11.51W					
13JUN78	48-12350-1	55.26N	8.24E					
13JUN78	48-12350-2	55.26N	8.24E					
14JUN78	49-12490-1	40.04N	9.38E					
14JUN78	49-12490-2	40.04N	9.38E					
14JUN78	49-12510-1	46.09N	7.40E					
14JUN78	49-12510-2	46.09N	7.40E					
14JUN78	49-12520-1	52.12N	5.20E					
14JUN78	49-12520-2	52.12N	5.20E					
15JUN78	50- 2090-3	55.49N	7.03E					
15JUN78	50- 2110-3	49.47N	4.25E					
15JUN78	50- 2120-3	43.42N	2.16E					
15JUN78	50- 2140-3	37.35N	.26E					

DATE	IDENTIFICATION	LOCATION		SCENE	SDE	ETAT	DST	PM
15JUN78	50-13070-1	40.05N	5.03E			C		
15JUN78	50-13100-1	52.13N	.46E					
15JUN78	50-13100-2	52.13N	.46E					
15JUN78	50-13120-2	58.14N	2.[illegible]					
16JUN78	51- 2270-3	56.20N	2.[illegible]					
16JUN78	51- 2320-3	38.07N	3.59W		307	R	M	8
16JUN78	51-13240-1	37.00N	1.23E			C		
16JUN78	51-13240-2	37.00N	1.23E			C		
16JUN78	51-13260-1	43.06N	.26E					
16JUN78	51-13260-2	43.06N	.26E					
16JUN78	51-13280-1	49.10N	2.34W					
16JUN78	51-13280-2	49.10N	2.34W					
17JUN78	52- 2450-3	55.38N	2.10W					
17JUN78	52- 2470-3	49.35N	4.47W					
17JUN78	52- 2490-3	43.31N	6.55W					
17JUN78	52-13430-1	37.35N	3.20W					
17JUN78	52-13460-1	49.45N	7.20W					
17JUN78	52-13460-2	49.45N	7.20W					
18JUN78	53- 3050-3	51.35N	8.33W			C		
18JUN78	53- 3060-3	45.31N	10.50W			C		
18JUN78	53-14030-1	46.05N	10.34W		305	R	M	8
18JUN78	53-14030-2	46.05N	10.34W		305	R	M	11
18JUN78	53-14050-1	52.09N	12.54W		305	R	M	2
18JUN78	53-14050-2	52.09N	12.54W		305	R	M	5
19JUN78	54- 1470-3	45.45N	8.58E		305	R	M	14
19JUN78	54- 1490-3	39.40N	7.02E		305	R	M	17
19JUN78	54-12430-1	42.46N	10.16E		294	R	M	23
19JUN78	54-12430-2	42.46N	10.16E		294	R	M	26
19JUN78	54-12450-1	48.51N	8.10E					
19JUN78	54-12450-2	48.51N	8.10E					
19JUN78	54-12470-1	54.53N	5.35E		321	R	M	20
19JUN78	54-12470-2	54.53N	5.35E		321	R	M	23
20JUN78	55- 2030-3	52.43N	7.05E					
20JUN78	55- 2030-3	52.58N	7.11E		296	R	M	26
20JUN78	55- 2040-3	52.00N	6.46E			C		
20JUN78	55- 2050-3	46.40N	4.43E			C		
20JUN78	55- 2050-3	45.56N	4.27E					
20JUN78	55- 2050-3	46.54N	4.47E		296	R	M	29
20JUN78	55- 2070-3	40.48N	2.47E					
20JUN78	55- 2070-3	40.34N	2.43E					
20JUN78	55- 2070-3	39.49N	2.30E			C		
20JUN78	55-13000-1	39.00N	6.50E		294	R	M	29
20JUN78	55-13000-2	39.00N	6.50E			C		
20JUN78	55-13020-1	45.05N	4.55E		295	R	M	2
20JUN78	55-13020-2	45.05N	4.55E		295	R	M	5
20JUN78	55-13040-1	51.10N	2.39E		295	R	M	8
20JUN78	55-13040-2	51.10N	2.39E		295	R	M	11
21JUN78	56- 2210-3	56.11N	4.04E					
21JUN78	56- 2220-3	50.09N	1.26E					
21JUN78	56- 2240-3	44.04N	.43E					

67

DATE	IDENTIFICATION	LOCATION		SCENE	BDE	ETAT	DST	PM
21JUN78	56- 2260-3	37.58N	2.34W		295	R	M	29
21JUN78	56-13180-1	36.42N	2.55E			C		
21JUN78	56-13180-2	36.42N	2.55E			C		
21JUN78	56-13190-1	42.49N	1.07E			C		
21JUN78	56-13190-2	42.49N	1.07E			C		
22JUN78	57-13350-1	35.02N	1.10W		321	R	M	26
22JUN78	57-13350-2	35.02N	1.10W		321	R	M	29
22JUN78	57-13370-1	41.08N	2.56W					
22JUN78	57-13370-2	41.08N	2.56W					
22JUN78	57-13390-1	47.13N	4.58W					
22JUN78	57-13390-2	47.13N	4.58W					
22JUN78	57-13400-1	53.17N	7.23W					
22JUN78	57-13400-2	53.47N	7.23W					
23JUN78	58- 2590-3	47.49N	8.34W					
23JUN78	58-13550-1	41.11N	7.30W					
23JUN78	58-13550-2	41.11N	7.30W					
23JUN78	58-13570-1	47.17N	9.31W					
23JUN78	58-13570-2	47.17N	9.31W					
24JUN78	59- 1410-3	42.31N	9.22E		322	R	M	2
24JUN78	59- 1430-3	36.24N	7.35E		322	R	M	5
24JUN78	59- 3160-3	52.22N	11.20W					
24JUN78	59- 3180-3	46.18N	13.40W					
24JUN78	59-12370-1	42.34N	11.47E		322	R	M	8
24JUN78	59-12370-2	42.34N	11.47E		322	R	M	11
24JUN78	59-12400-1	54.41N	7.07E					
24JUN78	59-12400-2	54.41N	7.07E					
25JUN78	60- 1560-3	54.26N	9.19E					
25JUN78	60- 1580-3	48.23N	6.49E					
25JUN78	60- 2000-3	42.17N	4.45E					
25JUN78	60- 2010-3	36.11N	2.59E					
25JUN78	60-12540-1	41.16N	7.39E					
25JUN78	60-12540-2	41.16N	7.39E					
25JUN78	60-12560-1	47.21N	5.38E					
25JUN78	60-12560-2	47.21N	5.38E					
26JUN78	61- 2160-3	49.14N	2.34E					
26JUN78	61- 2170-3	43.10N	.27E					
26JUN78	61- 2190-3	37.01N	1.20W		322	R	M	14
26JUN78	61-13110-1	36.55N	4.21E		322	R	M	17
26JUN78	61-13110-2	36.55N	4.21E		322	R	M	20
26JUN78	61-13130-1	43.01N	2.32E					
26JUN78	61-13130-2	43.01N	2.32E					
26JUN78	61-13150-1	49.06N	2.25E					
26JUN78	61-13150-2	49.06N	2.25E					
26JUN78	61-13160-1	55.08N	2.10W					
26JUN78	61-13160-2	55.08N	2.10W					
27JUN78	62-13290-1	35.01N	.19E		322	R	M	26
27JUN78	62-13290-2	35.01N	.19E		322	R	M	29
27JUN78	62-13300-1	41.08N	1.25W					
27JUN78	62-13300-2	41.08N	1.25W					
28JUN78	63- 2510-3	51.35N	5.36W					

DATE	IDENTIFICATION	LOCATION		SCENE	BDE	ETAT	DST	PM
28JUN78	63- 2530-3	45.32N	7.52W					
28JUN78	63-13490-1	43.33N	6.46W		323	R	M	2
28JUN78	63-13490-2	43.33N	6.46W		323	R	M	5
29JUN78	64-14080-1	44.41N	11.40W					
29JUN78	64-14080-2	44.41N	11.40W					
30JUN78	65- 1500-3	54.07N	10.39E					
30JUN78	65- 1530-3	41.59N	6.08E		305	R	M	20
30JUN78	65- 1550-3	35.53N	4.23E					
30JUN78	65-12470-1	39.22N	9.43E					
30JUN78	65-12470-2	39.22N	9.43E					
30JUN78	65-12490-1	45.29N	7.47E					
30JUN78	65-12490-2	45.49N	7.47E					
1JUL78	66-13050-1	38.10N	5.30E			C		
1JUL78	66-13050-2	38.10N	5.30E			C		
1JUL78	66-13080-1	50.21N	1.25E					
1JUL78	66-13080-2	50.21N	1.25E					
2JUL78	67- 2270-3	50.36N	.02E					
2JUL78	67- 2280-3	44.32N	2.09W					
2JUL78	67- 2300-3	38.26N	4.01W			C		
4JUL78	69-14000-1	41.18N	9.05W					
4JUL78	69-14000-2	41.18N	9.05W					
5JUL78	70- 1460-3	43.16N	8.04E					
5JUL78	70- 1460-3	42.29N	7.49E					
5JUL78	70- 1470-3	37.10N	6.15E					
5JUL78	70- 1480-3	36.23N	6.02E					
5JUL78	70-12410-1	43.01N	10.08E		332	R	M	26
5JUL78	70-12410-1	43.34N	9.58E					
5JUL78	70-12410-2	43.01N	10.08E		332	R	M	29
5JUL78	70-12410-2	43.34N	9.58E					
5JUL78	70-12450-1	55.09N	5.25E					
5JUL78	70-12450-1	55.41N	5.08E					
5JUL78	70-12450-2	55.09N	5.25E					
5JUL78	70-12450-2	55.41N	5.08E					
6JUL78	71- 2020-3	48.26N	5.17E					
6JUL78	71- 2040-3	42.22N	3.13E		305	R	M	23
6JUL78	71- 2060-3	36.16N	1.27E					
6JUL78	71-12570-1	36.10N	7.38E					
6JUL78	71-12570-2	36.10N	7.38E					
6JUL78	71-12590-1	42.16N	5.49E		323	R	M	8
6JUL78	71-12590-2	42.16N	5.49E		323	R	M	11
7JUL78	72- 2210-3	46.31N	.02E		295	R	M	14
7JUL78	72- 2230-3	40.25N	1.54W					
7JUL78	72-13170-1	40.08N	1.54E					
7JUL78	72-13170-1	40.05N	1.55E		295	R	M	17
7JUL78	72-13170-2	40.08N	1.54E					
7JUL78	72-13170-2	40.05N	1.55E		295	R	M	20
7JUL78	72-13180-1	46.14N	.03E					
7JUL78	72-13180-1	46.11N	.02E		295	R	M	23
7JUL78	72-13180-2	46.14N	.03E					
7JUL78	72-13180-2	46.11N	.02E		295	R	M	26

DATE	IDENTIFICATION	LOCATION		SCENE	BDE	ETAT	DST	PM
8JUL78	73- 2370-3	52.33N	2.10W					
8JUL78	73-13350-1	40.53N	2.50W					
8JUL78	73-13350-2	40.53N	2.50W					
8JUL78	73-13360-1	46.59N	4.51W		296	R	M	2
8JUL78	73-13360-2	46.59N	4.51W		296	R	M	5
10JUL78	75- 1390-3	42.20N	9.21E		296	R	M	8
10JUL78	75- 1410-3	36.14N	7.35E		296	R	M	11
10JUL78	75-12350-1	45.02N	11.01E		323	R	M	14
10JUL78	75-12350-2	45.02N	11.01E		323	R	M	17
10JUL78	75-12370-1	51.07N	8.46E					
10JUL78	75-12370-2	51.07N	8.46E					
11JUL78	76- 1540-3	52.29N	8.27E					
11JUL78	76- 1550-3	49.03N	7.04E					
11JUL78	76- 1560-3	46.26N	6.07E					
11JUL78	76- 1570-3	42.59N	4.58E		296	R	M	14
11JUL78	76- 1580-3	40.22N	4.10E			C		
11JUL78	76- 1590-3	36.53N	3.10E		296	R	M	17
11JUL78	76-12520-1	40.33N	7.52E		323	R	M	20
11JUL78	76-12520-2	40.33N	7.52E		323	R	M	23
11JUL78	76-12530-1	46.40N	5.54E					
11JUL78	76-12530-2	46.40N	5.54E					
11JUL78	76-12550-1	52.43N	3.32E					
11JUL78	76-12550-2	52.43N	3.32E					
12JUL78	77- 2130-3	51.37N	3.33E					
12JUL78	77- 2140-3	45.34N	1.17E		296	R	M	20
12JUL78	77- 2160-3	39.29N	.37E		296	R	M	23
13JUL78	78- 2310-3	51.45N	.56E					
13JUL78	78- 2320-3	45.42N	3.13W		322	R	M	23
16JUL78	81- 1500-3	45.08N	7.15E		323	R	M	26
16JUL78	81- 1510-3	39.04N	5.22E		323	R	M	29
17JUL78	82- 1540-3	.00N	.00E			C		
17JUL78	82- 2060-3	51.24N	5.02E					
17JUL78	82- 2080-3	45.21N	2.47E		297	R	M	2
17JUL78	82- 2090-3	39.17N	.53E					
17JUL78	82-13020-1	39.22N	5.15E			C		
17JUL78	82-13020-2	39.22N	5.15E			C		
17JUL78	82-13040-1	45.29N	3.19E			C		
17JUL78	82-13040-2	45.29N	3.19E			C		
17JUL78	82-13060-1	51.33N	1.07E					
17JUL78	82-13060-2	51.33N	1.02E					
18JUL78	83- 2270-3	39.41N	3.39W					
18JUL78	83- 2440-3	51.22N	.29E					
20JUL78	85- 3010-3	46.39N	10.22W					
21JUL78	86- 1450-3	36.18N	6.12E					
21JUL78	86-12380-1	42.55N	10.17E		297	R	M	5
21JUL78	86-12380-2	42.55N	10.17E		297	R	M	8
22JUL78	87- 2000-3	47.02N	4.59E					
22JUL78	87- 2020-3	40.58N	3.00E			L		
23JUL78	88- 2200-3	40.08N	1.47W					
25JUL78	90- 2530-3	51.47N	6.47W		324	R	M	2

DATE	IDENTIFICATION	LOCATION		SCENE	BDE	ETAT	DST	PM	
25JUL78	90- 2540-3	45.44N	9.04W		324	R	M	5	
26JUL78	91- 1370-3	41.00N	9.14E		297	R	M	11	
27JUL78	92- 1510-3	54.28N	9.41E						
27JUL78	92- 1530-3	48.27N	1.11E						
27JUL78	92- 1540-3	42.23N	5.07E		307	R	M	11	
27JUL78	92- 1560-3	36.19N	3.20E						
24SEP78	93- 2080-4	41.41N	6.03E		329	R	M	7	***
24SEP78	93- 2080-5	41.41N	6.03E		329	R	M	10	***
24SEP78	93- 2080-6	41.41N	6.03E		326	R	M	2	***
24SEP79	93- 2080-7	41.41N	6.03E		326	R	M	5	***
28JUL78	93- 2080-8	41.08N	.11E		329	R	M	4	***
28JUL78	93- 2100-3	50.54N	3.35E						
28JUL78	93- 2120-3	44.52N	1.22E			C			
28JUL78	93- 2130-3	58.47N	.30E						
28JUL78	93-13060-1	37.03N	4.29E		297	R	M	14	
28JUL78	93-13060-2	37.03N	4.29E		297	R	M	17	
28JUL78	93-13070-1	43.10N	2.40E		297	R	M	20	
28JUL78	93-13070-2	43.10N	2.40E		297	R	M	23	
28JUL78	93-13090-1	49.14N	.33E		297	R	M	26	
28JUL78	93-13090-2	49.14N	.33E		297	R	M	29	
28JUL78	93-13110-1	55.17N	2.01W						
28JUL78	93-13110-2	55.17N	2.01W						
29JUL78	94- 2280-3	51.50N	.31E		324	R	M	8	
29JUL78	94- 2290-3	45.48N	2.49W		324	R	M	11	
29JUL78	94-13230-1	36.00N	.16E						
29JUL78	94-13230-2	36.00N	.16E						
29JUL78	94-13250-1	42.07N	1.29W						
29JUL78	94-13250-2	42.07N	1.29W						
29JUL78	94-13270-1	48.11N	3.34W						
29JUL78	94-13270-2	48.11N	3.34W						
29JUL78	94-13280-1	54.14N	6.04W						
29JUL78	94-13280-2	54.14N	6.04W						
30JUL78	95- 2470-3	46.04N	7.16W						
30JUL78	95-13430-1	42.46N	6.16W						
30JUL78	95-13430-2	42.46N	6.16W						
30JUL78	95-13450-1	48.50N	8.22W						
30JUL78	95-13450-2	48.50N	8.22W						
31JUL78	96- 3040-3	51.54N	9.34W						
31JUL78	96- 3050-3	45.42N	11.52W						
31JUL78	96-12260-1	50.27N	10.45E						
31JUL78	96-12260-2	50.27N	10.45E						
31JUL78	96-12280-1	56.28N	8.01E						
31JUL78	96-12280-2	56.28N	8.01E						
31JUL78	96-14010-1	41.13N	10.17W						
31JUL78	96-14010-2	41.13N	10.17W						
31JUL78	96-14020-1	47.18N	12.19W						
31JUL78	96-14020-2	47.18N	12.19W						
1AUG78	97- 1470-3	43.46N	7.11E		296	R	M	2	
1AUG78	97- 1480-3	37.42N	5.21E						
5AUG78	101- 2590-3	46.08N	10.08W						

DATE	IDENTIFICATION	LOCATION		SCENE	BDL	ETAT	DST	PM
7AUG78	103- 1580-3	42.59N	4.01E					
7AUG78	103- 1590-3	36.54N	2.12E					
7AUG78	103-12520-1	39.58N	6.54E					
7AUG78	103-12520-2	39.58N	6.54E					
8AUG78	104- 2140-3	49.55N	1.57E					
8AUG78	104- 2150-3	43.52N	.12E					
8AUG78	104- 2170-3	37.47N	2.02W					
8AUG78	104-13100-1	39.41N	2.25E					
8AUG78	104-13100-2	39.41N	2.25E					
8AUG78	104-13120-1	45.46N	.29E					
8AUG78	104-13120-2	45.46N	.29E					
9AUG78	105-13290-1	44.46N	3.41W					
9AUG78	105-13290-2	44.46N	3.41W					
9AUG78	105-13310-1	50.50N	5.55W					
9AUG78	105-13310-2	50.50N	5.55W					
11AUG78	107- 1320-3	42.53N	10.11E					
11AUG78	107- 1340-3	36.48N	8.23E					
11AUG78	107- 3070-3	53.08N	10.17W					
11AUG78	107- 3090-3	47.07N	12.41W					
12AUG78	108- 1510-3	41.31N	5.13E			C		
12AUG78	108- 1530-3	35.26N	3.28E					
12AUG78	108-12450-1	40.34N	8.19E		324	R	M	20
12AUG78	108-12450-2	40.34N	8.19E		324	R	M	23
12AUG78	108-12470-1	46.39N	6.21E		324	R	M	14
12AUG78	108-12470-2	46.39N	6.21E		324	R	M	17
13AUG78	109- 2070-3	49.19N	3.22E					
13AUG78	109- 2080-3	43.17N	1.15E					
13AUG78	109- 2100-3	37.12N	.33E					
14AUG78	110- 2270-3	42.36N	3.29W			C		
14AUG78	110-13210-1	40.07N	.34E			C		
14AUG78	110-13210-2	40.07N	.34E			C		
14AUG78	110-13220-1	46.11N	2.31W			C		
14AUG78	110-13220-2	46.11N	2.31W			C		
17AUG78	113-12380-1	40.49N	9.54E		325	R	M	26
17AUG78	113-12390-1	42.16N	9.27E		324	R	M	26
17AUG78	113-12380-2	40.49N	9.54E		325	R	M	29
17AUG78	113-12380-2	42.16N	9.27E		324	R	M	29
17AUG78	113-12390-1	46.53N	7.55E					
17AUG78	113-12390-2	46.53N	7.55E					
17AUG78	113-12410-1	52.55N	5.31E		298	R	M	5
17AUG78	113-12410-2	52.55N	5.31E		298	R	M	8
18AUG78	114-12550-1	37.48N	6.16E		325	R	M	2
18AUG78	114-12550-2	37.48N	6.16E		325	R	M	5
18AUG78	114-12570-1	43.53N	4.25E		298	R	M	11
18AUG78	114-12570-2	43.53N	4.25E		298	R	M	14
19AUG78	115- 2170-3	51.58N	1.35E			C		
19AUG78	115- 2190-3	45.56N	.42E					
19AUG78	115- 2190-3	45.56N	.42E		307	R	[illegible]	14
19AUG78	115- 2200-3	39.52N	2.39W					
19AUG78	115-13130-1	37.32N	1.49E		325	R	[illegible]	6

DATE	IDENTIFICATION	LOCATION		SCENE	BDE	ETAT	DST	PM
19AUG78	115-13130-2	37.32N	1.49E		325	R	M	11
19AUG78	115-13140-1	43.37N	.00E		313	R	M	8
19AUG78	115-13140-2	43.37N	.00E		313	R	M	11
19AUG78	115-13160-1	49.40N	2.09W		313	R	M	2
19AUG78	115-13160-2	49.40N	2.09W		313	R	M	5
20AUG78	116- 2380-3	41.25N	4.43W					
20AUG78	116-13320-1	40.44N	3.38W					
20AUG78	116-13320-2	40.44N	3.38W					
20AUG78	116-13330-1	46.49N	5.37W					
20AUG78	116-13330-2	46.49N	5.37W					
20AUG78	116-13350-1	52.50N	8.00W					
20AUG78	116-13350-2	52.50N	8.00W					
21AUG78	117-13500-1	43.35N	9.04W		325	R	M	20
21AUG78	117-13500-2	43.35N	9.04W		325	R	M	23
21AUG78	117-13520-1	49.38N	11.13W		325	R	M	14
21AUG78	117-13520-2	49.38N	11.13W		325	R	M	17
22AUG78	118- 1350-3	45.16N	9.47E		290	R	M	17
22AUG78	118-12310-1	41.30N	11.21E		332	R	M	2
22AUG78	118-12310-2	41.30N	11.21E		332	R	M	5
22AUG78	118-12340-1	53.35N	6.53E					
22AUG78	118-12340-2	53.35N	6.53E					
23AUG78	119- 1510-3	54.52N	9.06E					
23AUG78	119- 1540-3	42.48N	4.26E					
23AUG78	119- 1560-3	36.43N	2.38E			C		
24AUG78	120- 2110-3	47.10N	1.22E					
24AUG78	120- 2120-3	41.06N	.37E			C		
24AUG78	120-13060-1	40.34N	2.34E		307	R	M	23
24AUG78	120-13060-2	40.34N	2.34E		307	R	M	26
24AUG78	120-13080-1	46.38N	.36E		307	R	M	17
24AUG78	120-13080-2	46.38N	.36E		307	R	M	20
25AUG78	121-13240-1	40.43N	2.01W			C		
25AUG78	121-13240-2	40.43N	2.01W			C		
25AUG78	121-13260-1	46.47N	4.00W			C		
25AUG78	121-13260-2	46.47N	4.00W			C		
25AUG78	121-13280-1	52.49N	6.22W					
25AUG78	121-13280-2	52.49N	6.22W					
26AUG78	122-13440-1	43.50N	7.34W			C		
26AUG78	122-13440-2	43.50N	7.34W			C		
26AUG78	122-13450-1	49.53N	9.43W			C		
26AUG78	122-13450-2	49.53N	9.43W			C		
27AUG78	123- 1290-3	44.15N	10.58E					
27AUG78	123- 1300-3	38.10N	9.05E					
28AUG78	124- 1460-3	49.26N	8.13E					
28AUG78	124-12410-1	39.00N	9.00E					
28AUG78	124-12410-2	39.00N	9.00E					
28AUG78	124-12430-1	45.05N	7.07E		298	R	M	20
28AUG78	124-12430-2	45.05N	7.07E		298	R	M	23
28AUG78	124-12450-1	51.07N	4.52E		298	R	M	26
28AUG78	124-12450-2	51.07N	4.52E		298	R	M	29
30AUG78	126-13180-1	40.44N	.41E			C		

DATE	IDENTIFICATION	LOCATION		SCENE	BDE	ETAT	DST	PM
30AUG78	126-13180-2	40.44N	.41E			C		
30AUG78	126-13200-1	46.47N	2.40W			C		
30AUG78	126-13200-2	46.47N	2.40W			C		
30AUG78	126-13220-1	52.49N	5.02W					
30AUG78	126-13220-2	52.49N	5.02W					
31AUG78	127- 2401-3	50.15N	5.14W			C		
31AUG78	127- 2421-3	44.12N	7.26W					
31AUG78	127-13380-1	45.05N	6.39W		308	R	M	17
31AUG78	127-13380-2	45.05N	6.39W		308	R	M	20
1SEP78	128-12220-1	56.23N	8.22E					
1SEP78	128-12220-2	56.23N	8.22E					
1SEP78	128-13550-1	41.23N	10.02W					
1SEP78	128-13550-2	41.23N	10.07W					
2SEP78	129- 1410-3	45.22N	8.06E		299	R	M	2
2SEP78	129- 1420-3	39.17N	6.11E					
2SEP78	129-12370-1	45.29N	8.19E			C		
2SEP78	129-12370-2	45.29N	8.19E			C		
3SEP78	130- 1590-3	42.55N	2.41E					
3SEP78	130-12540-1	38.57N	5.48E					
3SEP78	130-12540-2	38.57N	5.48E					
3SEP78	130-12550-1	45.01N	7.54E		308	R	M	8
3SEP78	130-12550-2	45.01N	7.54E		308	R	M	11
3SEP78	130-12570-1	51.04N	1.39E		308	IR		2
3SEP78	130-12570-2	51.04N	1.39E		308	R	M	5
4SEP78	131- 2150-3	51.40N	1.19E		308	R	M	14
4SEP78	131- 2170-3	45.37N	.58E					
5SEP78	132- 2340-3	50.22N	3.49W					
5SEP78	132- 2350-3	44.18N	6.02W					
5SEP78	132-13300-1	39.34N	3.32W					
5SEP78	132-13300-2	39.34N	3.32W					
6SEP78	133-13490-1	43.30N	9.20W					
6SEP78	133-13490-2	43.30N	9.20W					
7SEP78	134- 1370-3	35.29N	6.31E					
7SEP78	134- 3090-3	53.38N	11.36W					
7SEP78	134-12300-1	43.44N	10.16E					
7SEP78	134-12300-1	43.29N	10.21E					
7SEP78	134-12300-2	43.29N	10.21E					
7SEP78	134-12300-2	43.44N	10.16E					
7SEP78	134-12340-1	55.32N	5.35E					
7SEP78	134-12340-1	55.47N	5.29E					
7SEP78	134-12340-2	55.47N	5.29E					
7SEP78	134-12340-2	55.32N	5.35E					
8SEP78	135- 1550-3	36.49N	2.15E			C		
8SEP78	135-12470-1	37.32N	7.35E			C		
8SEP78	135-12470-2	37.32N	7.35E			C		
8SEP78	135-12490-1	47.37N	5.44E			C		
8SEP78	135-12490-2	47.37N	5.44E			C		
8SEP78	135-12500-1	49.40N	7.35E					
8SEP78	135-12500-2	49.40N	7.35E					
9SEP78	136- 2100-3	46.40N	.44E					

DATE	IDENTIFICATION	LOCATION		SCENE	BDE	ETAT	DST	PM
9SEP78	136- 2120-3	40.43N	1.14W					
9SEP78	136-13050-1	36.32N	3.17E			C		
9SEP78	136-13050-2	36.32N	3.17E			C		
9SEP78	136-13070-1	42.37N	1.29E			C		
9SEP78	136-13070-2	42.37N	1.29E			C		
9SEP78	136-13080-1	48.40N	.35E					
9SEP78	136-13080-2	48.40N	.35E					
10SEP78	137- 2290-3	44.37N	4.32W					
10SEP78	137-13240-1	40.06N	2.18W					
10SEP78	137-13240-2	40.06N	2.18W					
10SEP78	137-13260-1	46.10N	4.14W			C		
10SEP78	137-13260-2	46.10N	4.14W			C		
11SEP78	138- 2460-3	50.07N	7.07W					
12SEP78	139- 1290-3	42.48N	9.59E					
12SEP78	139- 1300-3	36.41N	8.11E					
13SEP78	140- 1450-3	51.05N	8.26E					
14SEP78	141- 2050-3	41.38N	.28E		309	R	M	20
14SEP78	141-12580-1	36.02N	4.49E					
14SEP78	141-12580-1	36.10N	4.47E		309	R	M	14
14SEP78	141-12580-2	36.02N	4.49E					
14SEP78	141-12580-2	36.10N	4.47E		309	R	M	17
14SEP78	141-13000-1	42.07N	3.02E					
14SEP78	141-13000-1	42.15N	3.00E		309	R	M	6
14SEP78	141-13000-2	42.07N	3.02E					
14SEP78	141-13000-2	42.15N	3.00E		309	R	M	11
14SEP78	141-13020-1	48.18N	.56E		309	R	M	2
14SEP78	141-13020-1	48.11N	.59E					
14SEP78	141-13020-2	48.11N	.59E					
14SEP78	141-13020-2	48.18N	.56E		309	R	M	5
14SEP78	141-13030-1	54.12N	1.30W					
14SEP78	141-13030-1	54.19N	1.33W					
14SEP78	141-13030-2	54.19N	1.33W					
14SEP78	141-13030-2	54.12N	1.30W					
15SEP78	142- 2210-3	52.02N	.22E					
15SEP78	142- 2210-3	51.55N	.25E		302	R	M	23
15SEP78	142- 2220-3	45.52N	2.43W			C		
15SEP78	142- 2220-3	45.59N	2.41W					
15SEP78	142-13180-1	40.21N	.58E		302	R	M	11
15SEP78	142-13180-2	40.21N	.58E		302	R	M	14
15SEP78	142-13190-1	46.25N	2.55W		302	R	M	17
15SEP78	142-13190-2	46.25N	2.55W		302	R	M	20
15SEP78	142-13210-1	52.27N	5.16W					
15SEP78	142-13210-2	52.27N	5.16W					
16SEP78	143- 2390-3	52.49N	4.34W					
16SEP78	143- 2400-3	46.46N	6.57W					
17SEP78	144-12210-1	55.17N	9.33E					
17SEP78	144-12210-2	55.17N	9.33E					
17SEP78	144-13560-1	46.05N	11.58W					
17SEP78	144-13560-2	46.05N	11.58W					
17SEP78	144-13570-1	52.08N	14.17W					

ORIGINAL PAGE IS
OF POOR QUALITY

DATE	IDENTIFICATION	LOCATION		SCENE	BDE	ETAT	DST	PM
17SEP78	144-13570-2	52.08N	14.17W					
18SEP78	145-12360-1	42.16N	9.00E		302	R	M	26
18SEP78	145-12360-2	42.16N	9.00E		302	R	M	29
18SEP78	145-12370-1	48.19N	6.56E					
18SEP78	145-12370-2	48.19N	6.56E					
18SEP78	145-12390-1	54.20N	4.26E					
18SEP78	145-12390-2	54.20N	4.26E					
19SEP78	146- 1570-3	50.44N	5.07E			C		
19SEP78	146- 1580-3	44.41N	2.53E			C		
19SEP78	146- 2000-3	38.35N	.59E			C		
21SEP78	148- 2340-3	45.48N	5.52W					
21SEP78	148-13280-1	36.19N	2.58W			C		
21SEP78	148-13280-2	36.19N	2.58W			C		
21SEP78	148-13300-1	42.25N	4.44W			C		
21SEP78	148-13300-2	42.25N	4.44W			C		
21SEP78	148-13320-1	48.28N	6.49W			C		
22SEP78	149- 2520-3	46.25N	10.13W			C		
22SEP78	149-13480-1	40.49N	8.49W			C		
22SEP78	149-13480-2	40.49N	8.49W			C		
22SEP78	149-13490-1	46.53N	10.48W			C		
22SEP78	149-13490-2	46.53N	10.48W			C		
23SEP78	150-12300-1	46.19N	9.07E					
23SEP78	150-12300-2	46.19N	9.07E					
23SEP78	150-12320-1	52.22N	6.47E					
24SEP78	151-12460-1	39.07N	6.50E					
24SEP78	151-12460-2	39.07N	6.50E					
24SEP78	151-12480-1	45.11N	4.56E					
24SEP78	151-12480-2	45.11N	4.56E					
24SEP78	151-12500-1	51.14N	2.41E					
24SEP78	151-12500-2	51.14N	2.41E					
25SEP78	152- 2080-3	50.33N	1.54E			C		
25SEP78	152- 2100-3	44.28N	.18E			C		
25SEP78	152- 2120-3	38.22N	2.11W			C		
26SEP78	153-13220-1	37.49N	1.54W					
26SEP78	153-13220-2	37.49N	1.54W					
26SEP78	153-13240-1	43.54N	3.45W		310	R	M	20
26SEP78	153-13240-2	43.54N	3.45W		310	R	M	23
26SEP78	153-13260-1	49.57N	5.55W		310	R	M	14
26SEP78	153-13260-2	49.57N	5.55W		310	R	M	17
27SEP78	154- 2450-3	49.29N	7.38W					
27SEP78	154- 2460-3	43.25N	9.47W					
27SEP78	154-13420-1	43.26N	8.09W			C		
27SEP78	154-13420-2	43.26N	8.09W			C		
28SEP78	155- 1280-3	42.18N	9.35E					
28SEP78	155- 1290-3	36.11N	7.48E					
28SEP78	155-12230-1	42.50N	11.44E					
28SEP78	155-12230-2	42.50N	11.44E					
28SEP78	155-12260-1	54.55N	7.05E					
28SEP78	155-12260-2	54.55N	7.05E					
29SEP78	156- 1460-3	41.52N	4.53E					

DATE	IDENTIFICATION	LOCATION		SCENE	BDE	ETAT	DST	PM
29SEP78	156- 1480-3	35.45N	3.07E					
29SEP78	156-12400-1	37.51N	8.40E			C		
29SEP78	156-12400-2	37.51N	8.40E			C		
29SEP78	156-12410-1	43.56N	6.49E			C		
29SEP78	156-12410-2	43.56N	6.49E			C		
30SEP78	157- 2030-3	44.17N	1.04E					
30SEP78	157- 2040-3	43.11N	.43E					
30SEP78	157- 2050-3	37.04N	1.05W					
30SEP78	157- 2050-3	38.10N	.47E					
2OCT78	159- 2400-3	44.11N	8.03W					
2OCT78	159-13360-1	44.32N	7.01W					
2OCT78	159-13360-2	44.32N	7.01W					
3OCT78	160-13530-1	43.29N	11.13W					
3OCT78	160-13530-2	43.29N	11.13W					
3OCT78	160-13550-1	49.32N	13.21W					
3OCT78	160-13550-2	49.32N	13.21W					
5OCT78	162-12520-1	40.38N	4.49E					
5OCT78	162-12520-2	40.38N	4.49E					
5OCT78	162-12530-1	46.43N	2.50E					
5OCT78	162-12530-2	46.43N	2.50E					
8OCT78	165-13460-1	42.28N	9.23W					
8OCT78	165-13460-2	42.28N	9.23W					
8OCT78	165-13480-1	48.32N	11.27W					
8OCT78	165-13480-2	48.32N	11.27W					
9OCT78	166-12270-1	41.44N	10.35E			C		
9OCT78	166-12270-2	41.44N	10.35E			C		
9OCT78	166-12290-1	47.49N	8.34E					
9OCT78	166-12290-2	47.49N	8.34E					
9OCT78	166-12300-1	53.52N	6.05E					
9OCT78	166-12300-2	53.52N	6.05E					
10OCT78	167-12450-1	39.56N	6.35E		299	R	M	5
10OCT78	167-12450-2	39.56N	6.35E		299	R	M	8
10OCT78	167-12460-1	46.02N	4.38E		299	R	M	23
10OCT78	167-12460-2	46.02N	4.38E		299	R	M	26
11OCT78	168- 2050-3	55.40N	4.09E					
11OCT78	168- 2060-3	49.37N	1.30E					
11OCT78	168- 2080-3	43.32N	.38E					
11OCT78	168- 2100-3	37.26N	2.28W					
11OCT78	168-13030-1	40.32N	1.52E					
11OCT78	168-13030-2	40.32N	1.52E					
11OCT78	168-13040-1	46.38N	.05E					
11OCT78	168-13040-2	46.38N	.05E					
11OCT78	168-13060-1	52.41N	2.27W					
11OCT78	168-13060-2	52.41N	2.27W					
12OCT78	169-13210-1	39.46N	2.26W					
12OCT78	169-13210-2	39.46N	2.26W					
12OCT78	169-13220-1	45.52N	4.22W					
12OCT78	169-13220-2	45.52N	4.22W					
12OCT78	169-13240-1	51.55N	6.40W					
12OCT78	169-13240-2	51.55N	6.40W					

DATE	IDENTIFICATION	LOCATION		SCENE	BDE	ETAT	DST	PM
130CT78	170-13390-1	41.38N	7.32W					
130CT78	170-13390-2	41.38N	7.32W					
130CT78	170-13410-1	47.43N	9.34W					
130CT78	170-13410-2	47.43N	9.34W					
140CT78	171-12210-1	43.46N	11.31E			C		
140CT78	171-12210-2	43.46N	11.31E			C		
140CT78	171-12220-1	49.51N	9.22E					
140CT78	171-12220-2	49.51N	9.22E					
150CT78	172-12380-1	41.04N	7.50E					
150CT78	172-12380-2	41.04N	7.50E					
150CT78	172-12400-1	47.09N	5.50E					
150CT78	172-12400-2	47.09N	5.50E					
160CT78	173-12550-1	37.14N	4.24E					
160CT78	173-12550-2	37.14N	4.24E					
160CT78	173-12570-1	43.20N	2.35E					
160CT78	173-12570-2	43.20N	2.35E					
170CT78	174-13140-1	39.54N	.53E					
170CT78	174-13140-1	39.43N	.50E					
170CT78	174-13140-2	39.54N	.53E					
170CT78	174-13140-2	39.43N	.50E					
170CT78	174-13170-1	52.04N	5.08W					
170CT78	174-13170-1	51.53N	5.04W					
170CT78	174-13170-2	52.04N	5.08W					
170CT78	174-13170-2	51.53N	5.04W					
180CT78	175-13320-1	42.42N	6.16W					
180CT78	175-13320-2	42.42N	6.16W					
190CT78	176-12150-1	51.03N	10.30E					
190CT78	176-12150-2	51.03N	10.30E					
200CT78	177-12320-1	47.28N	7.21E					
200CT78	177-12320-2	47.28N	7.21E					
210CT78	178-12480-1	39.02N	5.32E			C		
210CT78	178-12480-2	39.02N	5.32E			C		
210CT78	178-12500-1	45.08N	3.38E			C		
210CT78	178-12500-2	45.08N	3.38E			C		
220CT78	178-13080-1	46.28N	1.20W					
220CT78	178-13080-2	46.28N	1.20W					
220CT78	179-13060-1	40.22N	.37E			C		
220CT78	179-13060-2	40.22N	.37E			C		
230CT78	180- 2270-3	52.22N	3.10W					
240CT78	181-13430-1	42.10N	8.57W		305	R	M	27
240CT78	181-13430-2	42.10N	8.57W		305	R	M	30
240CT78	181-13450-1	48.15N	11.01W		308	R	M	23
240CT78	181-13450-2	48.15N	11.01W		308	R	M	26
250CT78	182-12231-1	41.37N	10.58E					
250CT78	182-12231-2	41.37N	10.58E					
250CT78	182-12250-1	48.04N	8.48E					
250CT78	182-12251-1	47.42N	8.56E					
250CT78	182-12251-2	47.42N	8.56E					
250CT78	182-12270-1	54.07N	6.19E					
250CT78	182-12270-2	54.07N	6.19E					

DATE	IDENTIFICATION	LOCATION		SCENE	BDE	ETAT	DST	PM
25OCT78	182-12271-1	53.46N	6.28E					
25OCT78	182-12271-2	53.46N	6.28E					
26OCT78	183-12410-1	38.50N	7.16E					
26OCT78	183-12410-2	38.50N	7.16E					
26OCT78	183-12420-1	44.57N	5.22E					
26OCT78	183-12420-2	44.57N	5.22E					
27OCT78	184-12580-1	35.14N	3.45E			C		
27OCT78	184-12580-2	35.14N	3.45E			C		
27OCT78	184-12590-1	41.22N	2.01E					
27OCT78	184-12590-2	41.22N	2.01E			C		
27OCT78	184-12590-3	40.45N	2.11E			C		
27OCT78	184-13010-1	47.28N	.00E			C		
27OCT78	184-13010-2	47.28N	.00E			C		
27OCT78	184-13010-3	46.51N	.13E					
27OCT78	184-13020-3	52.55N	2.10W					
27OCT78	184-13030-1	53.31N	2.26W					
27OCT78	184-13030-2	53.31N	2.26W					
28OCT78	185-13160-1	57.49N	1.26W		306	R	M	26
28OCT78	185-13160-2	57.49N	1.26W			C		
28OCT78	185-13180-1	43.56N	3.17W		306	R	M	8
28OCT78	185-13180-2	43.56N	3.17W		306	R	M	11
28OCT78	185-13200-1	50.01N	5.27W		306	R	M	2
28OCT78	185-13200-2	50.01N	5.27W		306	R	M	5
29OCT78	186-13360-1	45.09N	8.13W			C		
29OCT78	186-13360-2	45.09N	8.13W			C		
29OCT78	186-13380-1	51.13N	10.28W					
29OCT78	186-13380-2	51.13N	10.28W					
30OCT78	187-12170-1	44.34N	11.44E		309	R	M	23
30OCT78	187-12170-2	44.34N	11.44E		309	R	M	26
30OCT78	187-12180-1	50.38N	9.31E					
31OCT78	188- 1370-3	49.13N	8.01E					
31OCT78	188- 1390-3	43.08N	5.53E			C		
31OCT78	188- 1410-3	57.03N	4.04E			C		
1NOV78	189- 1550-3	51.14N	4.19E					
1NOV78	189- 1560-3	45.10N	2.04E			C		
1NOV78	189- 1580-3	57.05N	.08E			C		
1NOV78	189-12500-1	36.01N	5.17E			C		
1NOV78	189-12500-2	36.01N	5.17E			C		
1NOV78	189-12520-1	42.08N	3.31E			C		
1NOV78	189-12520-2	42.08N	3.31E			C		
1NOV78	189-12530-1	48.13N	1.28E			C		
1NOV78	189-12530-2	48.13N	1.28E			C		
1NOV78	189-12550-1	54.16N	1.02W					
1NOV78	189-12550-2	54.16N	1.02W					
2NOV78	190-13090-1	40.23N	.26E					
2NOV78	190-13090-2	40.23N	.26E					
2NOV78	190-13110-1	46.29N	2.24W		299	R	M	11
2NOV78	190-13110-2	46.29N	2.24W		299	R	M	14
2NOV78	190-13130-1	52.33N	4.46W					
2NOV78	190-13130-2	52.32N	4.46W					

ORIGINAL PAGE IS
OF POOR QUALITY

DATE	IDENTIFICATION	LOCATION		SCENE	BDE	ETAT	DST	PM
3NOV78	191-13280-1	45.13N	6.28W					
3NOV78	191-13280-2	45.13N	6.28W					
5NOV78	193-12260-1	40.37N	10.16E					
5NOV78	193-12260-2	40.37N	10.16E					
5NOV78	193-12270-1	46.43N	8.17E					
5NOV78	193-12270-2	46.43N	8.17E					
5NOV78	193-12290-1	52.47N	5.55E					
5NOV78	193-12290-2	52.47N	5.55E					
6NOV78	194-12430-1	38.22N	6.25E			C		
6NOV78	194-12430-2	38.22N	6.25E			C		
6NOV78	194-12450-1	44.29N	4.34E			C		
6NOV78	194-12450-2	44.29N	4.34E			C		
6NOV78	194-12460-1	50.34N	2.21E					
6NOV78	194-12460-2	50.34N	2.21E					
7NOV78	195- 2050-3	48.22N	.31E		310	R	M	8
7NOV78	195- 2050-3	48.50N	.41E		310	IP		2
7NOV78	195- 2070-3	42.17N	1.33W		310	R	M	11
7NOV78	195- 2070-3	42.47N	1.24W		310	R	M	5
7NOV78	195- 2080-3	36.41N	3.13W					
7NOV78	195-13010-1	40.49N	1.13E					
7NOV78	195-13010-2	40.49N	1.13E					
7NOV78	195-13030-1	46.55N	.45E					
7NOV78	195-13030-2	46.55N	.45E					
7NOV78	195-13050-1	52.59N	3.09W					
7NOV78	195-13050-2	52.59N	3.09W					
8NOV78	196- 2240-3	46.32N	4.36W					
9NOV78	197- 2400-3	52.53N	6.38W		306	R	M	29
9NOV78	197- 2420-3	46.52N	9.02W			C		
10NOV78	198- 1240-3	40.59N	8.43E					
10NOV78	198-12190-1	42.10N	11.25E					
10NOV78	198-12190-2	42.10N	11.25E					
10NOV78	198-12210-1	48.14N	9.21E					
10NOV78	198-12210-2	48.14N	9.21E					
11NOV78	199- 1420-3	44.27N	5.11E					
11NOV78	199- 1430-3	38.22N	7.19E					
11NOV78	199-12360-1	36.19N	8.31E					
11NOV78	199-12360-2	36.19N	8.31E					
11NOV78	199-12370-1	42.25N	6.43E					
11NOV78	199-12370-2	42.25N	6.43E					
11NOV78	199-12390-1	48.31N	4.38E					
11NOV78	199-12390-2	48.31N	4.38E					
11NOV78	199-12410-1	54.33N	2.07E					
11NOV78	199-12410-2	54.33N	2.07E					
12NOV78	200- 2000-3	44.50N	.43E		299	R	M	17
12NOV78	200- 2010-3	38.46N	1.10W		299	R	M	20
12NOV78	200-12540-1	35.33N	4.07E					
12NOV78	200-12540-2	35.33N	4.07E					
12NOV78	200-12550-1	41.40N	2.21E					
12NOV78	200-12550-2	41.40N	2.21E					
12NOV78	200-12570-1	47.46N	.19E		300	R	M	2

DATE	IDENTIFICATION	LOCATION		SCENE	BDE	ETAT	DST	PM	
12NOV78	200-12570-2	47.46N	.19E		300	R	M	5	
14NOV78	202-13330-1	45.35N	8.06W			C			
14NOV78	202-13330-2	45.35N	8.06W			C			
15NOV78	203- 1180-3	42.13N	10.22E			C			
15NOV78	203- 1200-3	36.08N	8.35E			C			
16NOV78	204- 1340-3	49.53N	8.28E						
16NOV78	204- 1360-3	43.50N	6.17E		300	R	M	8	
16NOV78	204- 1380-3	37.46N	4.26E						
17NOV78	205- 1520-3	51.40N	4.35E						
17NOV78	205- 1540-3	45.37N	2.17E		300	R	M	11	
19NOV78	207- 2290-3	50.32N	5.04W						
19NOV78	207- 2310-3	44.29N	7.17W			C			
21NOV78	209- 1310-3	39.49N	6.22E						
22NOV78	210- 1450-3	55.23N	7.38E						
22NOV78	210- 1470-3	49.23N	5.01E						
22NOV78	210- 1480-3	43.20N	2.52E			C			
22NOV78	210- 1500-3	37.16N	1.02E			C			
23NOV78	211- 2060-3	45.59N	.50E			C			
23NOV78	211- 2080-3	39.55N	2.46W						
24NOV78	212- 2230-3	48.37N	4.27W			C			
24NOV78	212- 2250-3	42.34N	6.32W						
28NOV78	216- 2020-3	37.38N	2.05W						
28NOV78	216-12540-1	36.58N	3.12E						
28NOV78	216-12540-1	36.39N	3.17E						
28NOV78	216-12540-2	36.58N	3.12E						
28NOV78	216-12540-2	36.39N	3.17E						
28NOV78	216-12560-1	43.05N	1.18E						
28NOV78	216-12560-1	42.47N	1.24E						
28NOV78	216-12560-2	43.05N	1.18E						
28NOV78	216-12560-2	42.47N	1.24E						
28NOV78	216-12570-1	48.50N	.39E		300	R	M	14	
28NOV78	216-12570-2	48.50N	.39E		300	R	M	17	
28NOV78	216-12580-1	49.09N	.46E						
28NOV78	216-12580-2	49.09N	.46E						
28NOV78	216-12590-1	54.52N	3.12W						
28NOV78	216-12590-2	54.52N	3.12W						
30NOV78	218- 2340-3	52.04N	6.16W						
30NOV78	218-13320-1	42.13N	7.32W						
30NOV78	218-13320-2	42.13N	7.32W						
30NOV78	218-13340-1	50.46N	10.33W		300	R	M	20	
30NOV78	218-13340-1	48.17N	9.35W		300	R	M	26	...
30NOV78	218-13340-2	50.46N	10.33W		300	R	M	23	
30NOV78	218-13340-2	43.17N	9.35W		300	R	H	29	...
5DEC78	223-13260-1	42.02N	6.01W						
5DEC78	223-13260-2	42.02N	6.01W						
6DEC78	224-12090-1	49.58N	10.45E						
6DEC78	224-12090-2	49.58N	10.54E						
6DEC78	224-12100-1	55.59N	9.14E						
6DEC78	224-12100-2	55.59N	9.14E						
6DEC78	224-13440-1	43.20N	11.02W						

DATE	IDENTIFICATION	LOCATION		SCENE	BDE	ETAT	DST	PM
6DEC78	224-13440-2	43.20N	11.02W					
6DEC78	224-13460-1	49.24N	13.10W					
6DEC78	224-13460-2	49.24N	13.10W					
7DEC78	225-12230-1	37.05N	10.32E					
7DEC78	225-12230-2	37.05N	10.32E					
7DEC78	225-12250-1	42.01N	9.05E		306	R	M	20
7DEC78	225-12250-1	43.11N	8.44E					
7DEC78	225-12250-2	42.01N	9.05E		306	R	M	23
7DEC78	225-12250-2	43.11N	8.44E					
7DEC78	225-12260-1	48.05N	7.02E					
7DEC78	225-12260-2	48.05N	7.02E					
7DEC78	225-12270-1	49.14N	6.37E					
7DEC78	225-12270-2	49.14N	6.37E					
7DEC78	225-12280-1	54.07N	4.34E		306	R	M	14
7DEC78	225-12280-2	54.07N	4.34E		306	R	M	17
8DEC78	226-12410-1	36.38N	6.06E					
8DEC78	226-12410-2	36.38N	6.06E					
9DEC78	227-12590-1	35.49N	1.46E					
9DEC78	227-12590-2	35.49N	1.46E					
9DEC78	227-13010-1	41.54N	.00E		301	R	M	2
9DEC78	227-13010-2	41.54N	.00E		301	R	M	5
9DEC78	227-13030-1	47.58N	2.01W		301	R	M	8
9DEC78	227-13030-2	47.58N	2.01W		301	R	M	11
9DEC78	227-13040-1	54.00N	4.29W					
9DEC78	227-13040-2	54.00N	4.29W					
10DEC78	228-13170-1	34.58N	2.34W					
10DEC78	228-13170-2	34.58N	2.34W					
10DEC78	228-13190-1	41.04N	4.17W					
10DEC78	228-13190-2	41.04N	4.17W					
10DEC78	228-13220-1	53.10N	8.41W					
10DEC78	228-13220-2	53.10N	8.41W					
11DEC78	229-13400-1	50.35N	12.09W					
11DEC78	229-13400-2	50.35N	12.09W					
13DEC78	231-12350-1	58.01N	7.11E			C		
13DEC78	231-12350-2	58.01N	7.11E			C		
14DEC78	232-12530-1	35.27N	3.20E					
14DEC78	232-12530-2	35.27N	3.20E					
14DEC78	232-12540-1	41.33N	1.35E					
14DEC78	232-12540-2	41.33N	1.35E					
14DEC78	232-12560-1	47.37N	.25E					
14DEC78	232-12560-2	47.37N	.25E					
14DEC78	232-12580-1	53.38N	2.50W					
14DEC78	232-12580-2	53.38N	2.50W					
16DEC78	234-13320-1	48.27N	9.50W					
16DEC78	234-13320-2	48.27N	9.50W					
17DEC78	235- 2520-2	50.40N	11.35W					
17DEC78	235- 2530-2	44.37N	13.49W					
17DEC78	235-12120-1	42.37N	11.53E					
17DEC78	235-12120-2	42.37N	11.53E					
17DEC78	235-12130-1	43.41N	9.49E					

DATE	IDENTIFICATION	LOCATION		SCENE	BDE	ETAT	DST	PM
17DEC78	235-12130-2	48.41N	9.49E					
17DEC78	235-12150-1	54.42N	7.17E					
17DEC78	235-12150-2	54.42N	7.17E					
18DEC78	236-12280-1	36.24N	9.10E					
18DEC78	236-12280-2	36.24N	9.10E					
18DEC78	236-12310-1	48.32N	5.19E					
18DEC78	236-12310-2	48.32N	5.19E					
18DEC78	236-12330-1	54.34N	2.47E					
18DEC78	236-12330-2	54.34N	2.47E					
19DEC78	237-12460-1	36.07N	4.41E					
19DEC78	237-12460-2	36.07N	4.41E					
19DEC78	237-12480-1	42.12N	2.55E					
19DEC78	237-12480-2	42.12N	2.55E					
19DEC78	237-12490-1	48.16N	.52E			C		
19DEC78	237-12490-2	48.16N	.52E			C		
19DEC78	237-12510-1	54.16N	1.36W			C		
19DEC78	237-12510-2	54.16N	1.36W			C		
20DEC78	238- 4380-2	37.20S	138.04E					
21DEC78	239- 2290-3	44.08N	7.54W					
21DEC78	239- 2290-3	43.49N	8.00W					
21DEC78	239-13250-1	45.08N	7.04W					
21DEC78	239-13250-2	45.08N	7.04W					
22DEC78	240-13440-1	49.37N	13.16W					
22DEC78	240-13440-2	49.37N	13.16W					
23DEC78	241-12230-1	42.34N	8.55E					
23DEC78	241-12230-2	42.34N	8.55E					
24DEC78	242-12400-1	39.18N	5.22E					
25DEC78	243- 2040-3	44.19N	1.42W		301	R	M	20
25DEC78	243-12580-1	39.57N	.37E					
25DEC78	243-12580-2	39.57N	.37E					
25DEC78	243-13000-1	46.01N	1.18W		301	R	M	14
25DEC78	243-13000-2	46.01N	1.18W		301	R	M	17
25DEC78	243-13020-1	52.04N	3.36W					
25DEC78	243-13020-2	52.04N	3.36W					
26DEC78	244- 2210-3	45.24N	5.53W		301	R	M	23
27DEC78	245- 2400-3	44.00N	10.55W					
28DEC78	246- 1210-3	40.52N	7.52E			C		
28DEC78	246-12160-1	43.31N	10.11E			C		
28DEC78	246-12160-2	43.31N	10.11E			C		
29DEC78	247- 1400-3	37.10N	2.14E					
29DEC78	247-12360-3	48.43N	3.51E					
29DEC78	247-12370-3	54.44N	1.19E					
30DEC78	248-12500-1	35.55N	3.20E					
30DEC78	248-12520-1	42.01N	1.36E					
30DEC78	248-[illegible]520-2	42.01N	1.36E					
31DEC78	249- [illegible]140-3	45.53N	4.07W					
31DEC78	249-13110-1	45.41N	4.07W					
31DEC78	249-13130-2	51.43N	6.24W					
3JAN79	252- 1320-3	41.33N	5.07E					
3JAN79	252- 1340-3	35.27N	7.22E					

83

DATE	IDENTIFICATION	LOCATION		SCENE	BDE	ETAT	DST	PM
3JAN79	252-12260-1	39.56N	8.25E					
3JAN79	252-12260-2	39.56N	8.25E					
3JAN79	252-12280-1	46.00N	6.29E					
3JAN79	252-12280-2	46.00N	6.29E					
3JAN79	252-12290-1	52.02N	4.11E					
3JAN79	252-12290-2	52.02N	4.11E					
6JAN79	255- 2260-3	42.50N	8.04W					
6JAN79	255-13210-1	44.07N	6.27W					
6JAN79	255-13210-2	44.07N	6.27W					
7JAN79	256- 1060-3	42.58N	11.44E					
7JAN79	256- 2410-3	53.41N	8.29W					
7JAN79	256-13390-1	43.02N	10.38W					
7JAN79	256-13390-2	43.02N	10.38W					
10JAN79	259- 1570-3	53.19N	2.31E					
10JAN79	259- 2010-3	41.10N	1.55W					
11JAN79	260- 2150-3	53.31N	1.49W					
12JAN79	261- 2330-3	54.42N	5.48W					
13JAN79	262- 1170-3	41.26N	8.50E	R	301	R	M	26
13JAN79	262- 1190-3	35.19N	7.04E					
13JAN79	262- 2520-3	50.31N	12.05W					
14JAN79	263- 1320-3	52.05N	8.13E		302	R	M	2
14JAN79	263- 1360-3	39.55N	7.55E		302	R	M	5
15JAN79	264- 1500-3	53.47N	4.25E					
15JAN79	264- 1510-3	47.44N	1.57E			C		
15JAN79	264- 1530-3	41.39N	.00E			C		
16JAN79	265- 2090-3	48.14N	2.15W			C		
16JAN79	265- 2110-3	42.10N	4.20W			C		
17JAN79	266- 2260-3	52.40N	4.57W					
17JAN79	266- 2270-3	46.37N	7.20W			C		
17JAN79	266-13230-1	40.42N	5.56W					
17JAN79	266-13230-2	40.42N	5.56W					
17JAN79	266-13250-1	46.46N	7.55W					
17JAN79	266-13250-2	46.46N	7.55W					
17JAN79	266-13260-1	52.49N	10.18W					
17JAN79	266-13260-2	52.49N	10.18W					
18JAN79	267-13420-1	42.58N	11.08W					
18JAN79	267-13420-2	42.58N	11.08W					
19JAN79	268- 1290-3	35.34N	4.32E					
21JAN79	270- 2010-3	51.18N	.36E					
21JAN79	270- 2010-3	51.18N	.36E					
21JAN79	270- 2030-3	45.14N	1.40W			C		
21JAN78	270- 2040-3	39.08N	3.35W					
21JAN79	270-13000-1	46.10N	1.36W					
21JAN79	270-13000-2	46.10N	1.36W					
21JAN79	270-13010-1	52.12N	3.56W					
21JAN79	270-13010-2	52.12N	3.56W					
23JAN79	272-12000-1	51.13N	11.05E					
23JAN79	272-12000-2	51.13N	11.05E					
23JAN79	272-13360-1	44.39N	10.47W					
23JAN79	272-13360-2	44.39N	10.47W					

DATE	IDENTIFICATION	LOCATION		SCENE	BDE	ETAT	DST	PM
23JAN79	272-13370-1	50.43N	13.01W					
23JAN79	272-13370-2	50.43N	13.01W					
24JAN79	273- 1210-3	41.20N	7.01E			C		
24JAN79	273- 1230-3	35.13N	5.16E					
25JAN79	274-12340-2	40.39N	5.33E					
25JAN79	274-12360-1	46.44N	3.34E					
25JAN79	274-12360-2	46.44N	3.34E					
25JAN79	274-12370-1	52.47N	1.11E					
25JAN79	274-12370-2	52.47N	1.11E					
26JAN79	275- 1590-3	38.38N	2.57W					
26JAN79	275-12520-1	39.40N	1.14E					
26JAN79	275-12520-2	39.40N	1.14E					
26JAN79	275-12550-1	51.49N	2.58W					
26JAN79	275-12550-2	51.49N	2.58W					
27JAN79	276- 2140-3	50.40N	3.29W					
28JAN79	277- 2330-3	47.36N	9.16W					
28JAN79	277-13300-1	44.29N	9.26W					
28JAN79	277-13300-2	44.29N	9.26W					
28JAN79	277-13320-1	50.33N	11.39W					
28JAN79	277-13320-2	50.33N	11.39W					
29JAN79	278- 1170-3	36.12N	6.51E					
30JAN79	279- 1320-3	43.00N	4.16E			C		
30JAN79	279- 1350-3	36.54N	2.28E			C		
30JAN79	279-12280-1	40.38N	6.51E					
30JAN79	279-12280-2	40.38N	6.51E					
31JAN79	280- 1490-3	51.37N	2.49E			C		
31JAN79	280- 1510-3	45.33N	.31E			C		
31JAN79	280- 1530-3	39.28N	1.23W			C		
1FEB79	281- 2060-3	51.26N	1.50W					
1FEB79	281- 2090-3	45.23N	4.07W					
2FEB79	282- 2261-3	49.15N	7.19W					
3FEB79	283- 1090-3	42.47N	10.08E					
3FEB79	283- 1110-3	36.41N	8.20E			C		
4FEB79	284- 1250-3	50.26N	8.16E					
4FEB79	284- 1270-3	44.22N	6.04E			C		
4FEB79	284- 1290-3	38.16N	4.11E			C		
4FEB79	284-12220-1	39.01N	8.41E			C		
4FEB79	284-12220-2	39.01N	8.41E			C		
5FEB79	285- 1430-3	50.50N	3.50E					
5FEB79	285- 1450-3	44.46N	1.37E					
5FEB79	285- 1470-3	38.41N	.16E					
5FEB79	285-12400-1	53.01N	4.24E			C		
5FEB79	285-12400-2	53.01N	4.24E			C		
5FEB79	285-12430-1	50.11N	.22E					
5FEB79	285-12430-2	50.11N	.22E					
6FEB79	286- 2010-3	53.41N	.28E			C		
6FEB79	286- 2020-3	47.38N	1.59W			C		
6FEB79	286-12570-1	36.03N	.20E					
6FEB79	286-12570-2	36.03N	.20E					
7FEB79	287-13160-1	39.37N	5.13W					

ORIGINAL PAGE IS
OF POOR QUALITY

85

DATE	IDENTIFICATION	LOCATION		SCENE	DDE	ETAT	DST	PM
7FEB79	287-13160-2	39.37N	5.13W					
7FEB79	287-13180-1	45.43N	7.08W					
7FEB79	287-13180-2	45.43N	7.08W					
10FEB79	290- 1370-3	49.51N	5.27[illegible]					
14FEB79	294-12090-1	42.04N	11.14E					
14FEB79	294-12090-2	42.04N	11.14E					
15FEB79	295-12260-1	38.46N	7.40E					
15FEB79	295-12260-2	38.46N	7.40E					
16FEB79	296-12450-1	40.41N	2.32E					
17FEB79	297-13020-1	38.04N	1.13W					
17FEB79	297-13020-2	38.04N	1.13W					
17FEB79	297-13040-1	44.10N	3.04W					
17FEB79	297-13040-2	44.10N	3.04W					
20FEB79	300-12190-1	38.49N	9.13E					
20FEB79	300-12190-2	38.49N	9.13E					
20FEB79	300-12210-1	44.55N	7.20E					
20FEB79	300-12210-2	44.55N	7.20E					
20FEB79	300-12230-1	50.59N	5.05E					
20FEB79	300-12230-2	50.59N	5.05E					
21FEB79	301-12380-1	41.35N	3.53E			C		
21FEB79	301-12380-2	41.35N	3.53E			C		
21FEB79	301-12400-1	47.40N	1.50E			C		
21FEB79	301-12400-2	47.40N	1.50E			C		
22FEB79	302-12550-1	38.53N	.08E					
22FEB79	302-12550-2	38.53N	.08E			C		
22FEB79	302-12590-1	51.04N	4.00W			C		
22FEB79	302-12590-2	51.04N	4.00W					
23FEB79	303-13150-1	44.11N	6.00W			C		
23FEB79	303-13150-2	44.11N	6.00W			C		
23FEB79	303-13160-1	50.16N	8.12W			C		
23FEB79	303-13160-2	50.16N	8.12W			C		
24FEB79	304-11580-1	52.42N	10.33E					
24FEB79	304-11580-2	52.42N	10.33E					
24FEB79	304-13330-1	44.39N	10.40W					
24FEB79	304-13330-2	44.39N	10.40W					
25FEB79	305-12130-1	42.46N	9.42E					
25FEB79	305-12130-2	42.46N	9.42E					
25FEB79	305-12150-1	48.52N	7.36E					
25FEB79	305-12150-2	48.52N	7.36E					
25FEB79	305-12160-1	54.54N	5.02E					
25FEB79	305-12160-2	54.54N	5.02E					
26FEB79	306-12300-1	39.14N	6.16E					
26FEB79	306-12300-2	39.14N	6.16E					
26FEB79	306-12320-1	45.20N	4.21E					
26FEB79	306-12320-2	45.20N	4.21E					
26FEB79	306-12330-1	51.24N	2.04E					
26FEB79	306-12330-2	51.24N	2.04E					
27FEB79	307- 1530-3	45.35N	.51E			C		
27FEB79	307- 1550-3	39.30N	2.46W					
27FEB79	307-12480-1	38.01N	2.06E					

DATE	IDENTIFICATION	LOCATION		SCENE	BDE	ETAT	DST	PM
27FEB79	307-12480-2	38.01N	2.06E					
27FEB79	307-12490-1	44.07N	.14E			C		
27FEB79	307-12490-2	44.07N	.14E			C		
27FEB79	307-12510-1	50.11N	1.56W			C		
27FEB79	307-12510-2	50.11N	1.56W			C		
1MAR79	309-13250-1	45.01N	9.03W					
1MAR79	309-13250-2	45.01N	9.03W					
14MAR79	322-12270-1	38.42N	6.07E			C		
14MAR79	322-12270-2	38.42N	6.07E			C		
14MAR79	322-12290-2	44.47N	4.13E			C		
15MAR79	323-12460-1	39.55N	1.08E					
15MAR79	323-12460-2	39.55N	1.08E					
16MAR79	324-13040-1	39.04N	3.11W					
16MAR79	324-13040-2	39.04N	3.11W					
16MAR79	324-13050-1	45.09N	5.05W			C		
16MAR79	324-13050-2	45.09N	5.05W			C		
17MAR79	325-13230-1	41.02N	8.20W					
17MAR79	325-13230-2	41.02N	8.20W					
17MAR79	325-13240-1	47.07N	10.20W					
17MAR79	325-13240-2	47.07N	10.20W					
18MAR79	326-12040-1	43.29N	10.35E			C		
18MAR79	326-12040-2	43.29N	10.35E			C		
18MAR79	326-12080-1	55.34N	5.50E					
18MAR79	326-12080-2	55.34N	5.50E					
19MAR79	327-12210-1	37.19N	7.52E			C		
19MAR79	327-12210-2	37.19N	7.52E			C		
19MAR79	327-12220-1	43.25N	6.03E					
19MAR79	327-12220-2	43.25N	6.03E					
19MAR79	327-12260-1	55.30N	1.17E					
19MAR79	327-12760-2	55.30N	1.17E					
20MAR79	328-12390-1	36.41N	3.28E			C		
20MAR79	328-12390-2	36.41N	3.28E			C		
20MAR79	328-12400-1	42.47N	1.40E			C		
20MAR79	328-12400-2	42.47N	1.40E			C		
20MAR79	328-12420-1	48.51N	.25E			C		
20MAR79	328-12420-2	48.51N	.25E			C		
21MAR79	329-12570-1	38.56N	1.43W					
21MAR79	329-12570-2	38.56N	1.43W					
21MAR79	329-12590-1	45.01N	3.37W					
21MAR79	329-12590-2	45.01N	3.37W					
21MAR79	329-13010-1	51.04N	5.51W					
21MAR79	329-13010-2	51.04N	5.51W					
23MAR79	331-11580-1	43.29N	12.02E					
23MAR79	331-11580-2	43.29N	12.02E					
23MAR79	331-11590-1	49.32N	9.53E					
23MAR79	331-11590-2	49.32N	9.53E					
23MAR79	331-12010-1	55.34N	7.16E			C		
23MAR79	331-12010-2	55.34N	7.16E			C		
24MAR79	332-12150-1	39.07N	8.49E			C		
24MAR79	332-12150-2	39.07N	8.49E			C		

87

DATE	IDENTIFICATION	LOCATION		SCENE	BDE	ETAT	DST	PM
24MAR79	332-12160-1	45.12N	6.56E			C		
24MAR79	332-12160-2	45.12N	6.56E			C		
24MAR79	332-12180-1	51.15N	4.41E			C		
24MAR79	332-12180-2	51.15N	4.41E			C		
25MAR79	333-12330-1	38.09N	4.32E					
25MAR79	333-12330-2	38.09N	4.32E					
26MAR79	334-12530-1	46.59N	2.47W					
26MAR79	334-12530-2	46.59N	2.47W					
27MAR79	335-13090-1	39.46N	5.00W					
27MAR79	335-13090-2	39.46N	5.00W					
30MAR79	338-12260-1	38.02N	6.10E					
30MAR79	338-12260-2	38.02N	6.10E					
30MAR79	338-12270-1	44.07N	4.19E					
30MAR79	338-12270-2	44.07N	4.19E					
1APR79	340-13010-1	37.32N	2.13W					
1APR79	340-13010-2	37.32N	2.13W					
1APR79	340-13030-1	43.37N	4.04W					
1APR79	340-13030-2	43.37N	4.04W					
1APR79	340-13050-1	49.40N	6.14W					
1APR79	340-13050-2	49.40N	6.14W					
2APR79	341-13210-1	41.59N	8.05W					
2APR79	341-13210-2	41.59N	8.05W					
2APR79	341-13220-1	48.03N	10.08W					
2APR79	341-13220-2	48.03N	10.08W					
7APR79	346-13130-1	43.41N	7.21W					
7APR79	346-13130-2	43.41N	7.21W					
7APR79	346-13150-1	49.45N	9.31W					
7APR79	346-13150-2	49.45N	9.31W					
8APR79	347- 590-3	41.38N	10.23E		302	R	M	6
8APR79	347-13330-1	49.01N	13.43W					
8APR79	347-13330-2	49.01N	13.43W					
10APR79	349-12290-1	39.14N	4.48E					
10APR79	349-12290-2	39.14N	4.48E					
10APR79	349-12320-1	51.22N	.37E			C		
10APR79	349-12320-2	51.22N	.37E			C		
11APR79	350-12460-1	39.40N	.11E					
11APR79	350-12460-2	39.40N	.11E					
11APR79	350-12480-1	45.45N	1.44W					
11APR79	350-12480-2	45.45N	1.44W					
12APR79	351-13050-1	39.13N	4.18W					
12APR79	351-13050-2	39.13N	4.18W					
12APR79	351-13060-1	45.17N	6.12W			C		
12APR79	351-13060-2	45.17N	6.12W			C		
13APR79	352-11490-1	50.39N	11.28E					
13APR79	352-11490-2	50.39N	11.28E					
13APR79	352-11500-1	53.04N	10.26E					
13APR79	352-11500-2	53.04N	10.26E					
13APR79	352-11510-1	56.40N	8.43E					
13APR79	352-11510-2	56.40N	8.43E					
17APR79	356-13000-1	39.13N	3.11W			C		

88

DATE	IDENTIFICATION	LOCATION		SCENE	BDE	ETAT	DST	PM
17APR79	356-13000-2	59.13N	3.11W			C		
17APR79	356-13010-1	45.17N	5.06W			C		
17APR79	356-13010-2	45.17N	5.06W					
17APR79	356-13030-1	51.20N	7.22W			C		
17APR79	356-13030-2	51.20N	7.22W			C		
18APR79	357-13200-1	45.06N	9.41W					
18APR79	357-13200-2	45.06N	9.41W					
19APR79	358-12000-1	41.25N	11.10E					
19APR79	358-12000-2	41.25N	11.10E					
19APR79	358-12030-1	53.30N	6.43E					
19APR79	358-12030-2	53.30N	6.43E					
21APR79	360-12370-1	40.30N	2.10E					
21APR79	360-12370-2	40.30N	2.10E					
23APR79	362-13160-1	49.34N	10.08W					
23APR79	362-13160-2	49.34N	10.08W					
25APR79	364- 1160-3	50.47N	8.08E					
25APR79	364- 1180-3	44.43N	5.56E			C		
26APR79	365- 1350-3	48.31N	2.40E					
26APR79	365- 1370-3	42.26N	.35E					
26APR79	365-12310-1	40.06N	3.28E			C		
26APR79	365-12310-2	40.06N	3.28E			C		
26APR79	365-12330-1	46.10N	1.32E					
26APR79	365-12330-2	46.10N	1.32E					
26APR79	365-12340-1	52.13N	.47E					
29APR79	368- 540-3	43.11N	11.18E					
1MAY79	370- 1310-3	41.56N	1.40E			C		
1MAY79	370-12250-1	37.28N	5.29E		332	R	M	20
1MAY79	370-12250-2	37.28N	5.29E		332	R	M	23
1MAY79	370-12260-1	43.34N	3.38E		332	R	M	14
1MAY79	370-12260-2	43.34N	3.38E		332	R	M	17
2MAY79	371- 1480-3	46.58N	1.15W					
2MAY79	371- 1500-3	40.53N	3.14W					
3MAY79	372- 2040-3	55.53N	2.08W					
3MAY79	372- 2060-3	49.50N	4.47W					
5MAY79	374- 1060-3	45.37N	8.46E			C		
6MAY79	375- 1230-3	50.43N	6.04E					
6MAY79	375- 1250-3	44.38N	3.51E			C		
6MAY79	375-12200-1	39.50N	6.04E		332	R	M	8
6MAY79	375-12200-2	39.50N	6.04E		332	R	M	11
6MAY79	375-12210-1	45.56N	4.08E					
6MAY79	375-12210-2	45.56N	4.08E					
7MAY79	376- 1420-3	46.56N	.01E			C		
7MAY79	376- 1440-3	40.50N	1.57W					
7MAY79	376-12380-1	41.03N	1.09E			C		
7MAY79	376-12380-2	41.03N	1.09E			C		
8MAY79	377- 2000-3	48.56N	3.50W					
10MAY79	379- 1010-3	41.72N	6.48E			C		
11MAY79	380- 1180-3	45.22N	5.26E			C		
11MAY79	380-12130-1	38.41N	7.46E			C		
11MAY79	380-12130-2	38.41N	7.46E			C		

DATE	IDENTIFICATION	LOCATION		SCENE	BDE	ETAT	DST	PN
11MAY79	380-12150-1	44.46N	5.53E			C		
11MAY79	380-12150-2	44.46N	5.53E			C		